

Time-Domain Response of Multiconductor Transmission Lines

Djordjevic, A.R.; Sarkar, T.K.; Harrington, R.F.;

© 1987 IEEE. Personal use of this material is permitted. Permission from IEEE must be obtained for all other uses, in any current or future media, including reprinting/republishing this material for advertising or promotional purposes, creating new collective works, for resale or redistribution to servers or lists, or reuse of any copyrighted component of this work in other works.

Abstract available at: http://ieeexplore.ieee.org/xpl/freeabs_all.jsp?arnumber=1458064

This paper appears in: [Proceedings of the IEEE](#)

Issue Date: June 1987

Volume: 75 [Issue:6](#)

On page(s): 743 - 764

ISSN: 0018-9219

Cited by : 17

Digital Object Identifier: [10.1109/PROC.1987.13797](https://doi.org/10.1109/PROC.1987.13797)

Date of Current Version: 28 June 2005

Sponsored by: [IEEE](#)

Time-Domain Response of Multiconductor Transmission Lines

ANTONIJE R. DJORDJEVIĆ, TAPAN K. SARKAR, SENIOR MEMBER, IEEE,
AND ROGER F. HARRINGTON, FELLOW, IEEE

Evaluation of the time-domain response of multiconductor transmission lines is of great importance in the analysis of the crosstalk in fast digital circuit interconnections, as well as in the analysis of power lines. Several techniques for the computation of the line response, starting from the known circuit-theory parameters, are presented and evaluated. These methods are: time-stepping solution of the telegrapher equations, modal analysis in the time domain, model analysis in the frequency domain, and a convolution technique which uses line Green's functions. The last method can treat the most general case of lossy transmission lines with nonlinear terminal networks. Numerical and experimental results are presented to illustrate these techniques and to give insight into the crosstalk problems in fast digital circuits.

I. INTRODUCTION

The purpose of this paper is to present and compare several methods for the analysis of multiconductor transmission line response. This response is of great interest in modern, fast computers, where signals are carried from one chip to another along buses, which are transmission lines with many conductors, and they are most frequently fabricated on printed-circuit boards. The signals suffer certain distortions along the line, which might degrade the performance of fast computers. A knowledge of the line response is essential for the design of the signal paths in such cases. A transient analysis of multiconductor transmission lines is also important for power systems, where it is used to predict the behavior of long power lines excited by lightning strokes, or under other disruptions, such as a short circuit at some place. However, our principal concern is with the printed-circuit lines, although the techniques presented below can be applied to other multiconductor transmission lines.

A rigorous analysis of a multiconductor transmission line

is very involved, especially if the response at high frequencies (usually, in the gigahertz region) is to be properly evaluated. First, a real multiconductor transmission line is most frequently embedded in an inhomogeneous medium, and thus the waves that propagate along the line are not of the transverse electromagnetic (TEM) nature. However, even if the medium is homogeneous, due to the losses in the conductors, the line cannot support TEM waves. At very high frequencies (in the microwave region), the cross-sectional dimensions of the line become comparable to the wavelength, and higher order (again, non-TEM) modes can propagate. Secondly, the analysis is complicated by having to include the influence of discontinuities, present at line ends, bends, crossovers, etc. Finally, in order to evaluate the response of a transmission line terminated by arbitrary networks, which are, generally, nonlinear (e.g., active components) and with memory (i.e., contain capacitors and inductors), one has to consider the whole system simultaneously.

Perhaps the most general approach to evaluating the time-domain response of any electromagnetic system (such as a transmission line, or an antenna) is to solve Maxwell's equations in the time domain, or to utilize certain integro-differential equations which stem from Maxwell's equations [1]. Such a procedure could, in principle, take into account all the effects of the system geometry and electrical properties, and also include nonlinearities. However, such a method would be rather involved even for the simpler structures, and very hard to implement even on very large and powerful computers. Therefore, certain approximations are usually introduced, which greatly simplify the analysis.

First, we are going to consider the multiconductor transmission line to be uniform along its length. At the ends, the line is terminated by arbitrary networks. If the line has some discontinuities along its length, it can be divided into a number of uniform sections and the effects of the discontinuities can be taken into account by introducing suitable equivalent networks, such as those listed in [2] for microstrip lines.

Secondly, we are going to assume that the line behavior can completely be described in terms of circuit-theory parameters, i.e., in terms of matrices of inductances, capac-

Manuscript received December 13, 1985; revised December 29, 1986. This paper was supported in part by the Digital Equipment Corporation and by E. I. Du Pont De Nemours & Co. The submission of this paper was encouraged after review of an advance proposal.

A. R. Djordjević is with the Department of Electrical Engineering, University of Belgrade, 11001 Belgrade, Yugoslavia.

T. K. Sarkar and R. F. Harrington are with the Department of Electrical and Computer Engineering, Syracuse University, Syracuse, NY 13210, USA.

IEEE Log Number 8714146.

0018-9219/87/0600-0743\$01.00 © 1987 IEEE

stances, resistances, and conductances per unit length [3]. These parameters can be frequency-dependent (e.g., due to skin effect, or due to dielectric losses), although they are often taken to be constant. In the present paper, we are not going to discuss the evaluation of these parameters, i.e., these parameters are assumed to be known. The analysis which is based on the circuit-theory parameters is usually referred to as quasi-TEM analysis, because we have to assume the wave propagation along the line to be of a quasi-TEM nature in order to be able to define the line circuit-theory parameters.

With these assumptions, the multiconductor transmission line can be described by a system of partial differential equations in the time domain or by a system of ordinary differential equations in the frequency domain. These equations are given in the second section.

There are several methods of solving these equations. The conceptually simplest, but usually least efficient technique, is the time-stepping method. It can be applied to multiconductor transmission lines with frequency-independent parameters and with arbitrary terminal networks. This method is presented in the third section.

Along a transmission line with N signal conductors and one return conductor (the ground), generally N different quasi-TEM modes can propagate (at any frequency). For a lossless line (with frequency-independent parameters), such modes exist in the time domain, and they can also be defined in the frequency domain. However, for a lossy line, in the general case, the modes can be defined in the frequency domain only. Modal analysis is a very efficient technique for evaluating the response of a multiconductor transmission line. It is presented in the fourth and fifth sections of the paper, for the time domain and for the frequency domain, respectively.

A particular problem in the analysis of multiconductor transmission lines is the inclusion of the terminal network analysis. If these networks are linear, the analysis can be performed either in the time domain, or in the frequency domain. In the latter case, the Fourier transform may be used to switch between the time domain and the frequency domain. If the line is lossless, with frequency-independent parameters, the entire analysis can be performed in the time domain. In other cases the analysis must be performed in the frequency domain. Problems arise when the terminal networks are nonlinear. In the general case, such networks can be analyzed only in the time domain. In contrast, in some cases the analysis of the line has to be performed in the frequency domain. A way of combining these two solutions which enables the analysis of lossy lines (or lines with frequency-dependent parameters) with nonlinear terminal networks is presented in the sixth section.

In the seventh section several examples of the analysis of multiconductor transmission lines are given. In one case they are compared to experimentally obtained data.

Finally, in the eighth section, the various techniques for the multiconductor transmission line analysis are evaluated and compared.

The beginnings of transmission line analysis go back to 1883 [4]. In 1926 weakly coupled lines were analyzed [5], and in 1937 and 1941 a rigorous theory of coupled lines was given in terms of matrix equations [6], [7]. A modal theory of a pair of coupled lines was established in 1947 [8]. A justification of the quasi-TEM approximation of transmission lines can be found in [9].

The analysis of multiconductor transmission lines has found its most important applications in power distribution systems, in the analysis of crosstalk in fast digital circuits, in microwave theory [10]–[28], and in EMP (electromagnetic pulse) investigations. In many papers, computer algorithms are proposed for evaluation of the response of multiconductor transmission lines. In [23] and [27], two lumped-element models are considered. In [13], [19], and [21], computer-oriented models of lossless lines are described, while [15], [16], [23], and [28] give methods for the analysis of lines with frequency-dependent losses. Some of the latter techniques are based on the inverse Fourier transform, e.g., [15], while others include the convolution integral, e.g., [16]. In [17], a treatment of nonlinear systems is given. In [24], the theory of lossy multiconductor transmission lines is efficiently applied to the analysis of interdigital and similar microwave filters. Of course, the above list of references is by no means exhaustive.

II. QUASI-TEM EQUATIONS FOR MULTICONDUCTOR TRANSMISSION LINES

Let us consider a transmission line having a total of $(N + 1)$ conductors (Fig. 1). We assume that N conductors are signal conductors, and conductor number $(N + 1)$ is the

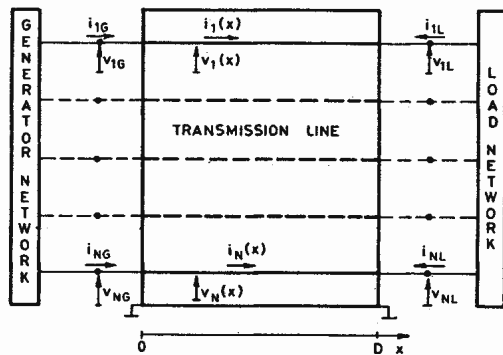


Fig. 1. Sketch of a multiconductor transmission line with terminal networks.

ground (reference) conductor. We further assume that the ground is at zero potential. The transmission line is assumed to be of an arbitrary cross section, but uniform along its length. Let the x -axis be oriented along the length of the transmission line, with $x = 0$ corresponding to the generator position, and $x = D$ corresponding to the load position. If the line dielectric is homogeneous, and if the conductors are lossless, the transmission line can support the so-called TEM waves at any frequency. A fundamental property of these waves is that the electric-field vector \vec{E} and the magnetic-field vector \vec{H} have only components perpendicular to the direction of propagation along the line. In other words, for these waves $E_x = 0$ and $H_x = 0$. Strictly speaking, in the presence of inhomogeneous dielectrics and/or losses in the line conductors, the waves that propagate along the line cannot be of a TEM type. They are, generally, of a hybrid nature (i.e., a combination of TE and TM modes). These waves have $E_x \neq 0$ and $H_x \neq 0$. However, for suitable dimensions of the transmission line (i.e., for the maximal cross-sectional dimensions of the line sufficiently smaller than the wavelength of the highest frequency component of interest), the longitudinal field components are much

smaller than the transversal components. Therefore, these hybrid waves can be approximated by TEM waves, which are, more precisely, called quasi-TEM waves. We shall assume throughout the analysis that we have only the quasi-TEM propagation.

Quasi-TEM wave propagation can be analyzed either starting from field theory, i.e., from Maxwell's equations, or starting from distributed-circuit parameters. These two approaches yield practically identical results for low-loss lines not at extremely high frequencies, which is the case considered here. For a more detailed treatment of this problem, refer to [29].

In the analysis we assume that we know the matrices of the line circuit-theory parameters, namely, that we know the following $N \times N$ matrices: matrix $[L]$ of inductances per unit length, matrix $[R]$ of resistances per unit length, matrix $[B]$ of electrostatic induction coefficients per unit length, and matrix $[G]$ of conductances per unit length. Note that the elements of matrix $[B]$ are frequently referred to as the capacitance coefficients. However, these coefficients are not equal to the self- and mutual capacitances between the conductors, and the term "capacitance coefficients" might be confusing. The self-capacitance of the k th conductor equals the sum of the electrostatic induction coefficients in the k th row of matrix $[B]$, while the mutual capacitance between the k th and ℓ th conductor equals the negative of the coefficient $B_{k\ell}$ of matrix $[B]$. Note that the mutual capacitances are always positive, while the off-diagonal coefficients of the $[B]$ matrix are always negative.

Let $v_k(x, t)$ represent the voltage between the k th signal conductor and ground at a distance x from the generator end and at a particular time instant t . Let $i_k(x, t)$ be the current flowing through the k th conductor, at a distance x from the generator end and at a particular time instant t . It is assumed that the reference direction of the current is from the generator to the load end. It is well known from circuit theory that the voltages and currents along a transmission line for the TEM mode of propagation are related by the telegrapher equations

$$\begin{aligned} \frac{\partial v_k(x, t)}{\partial x} &= - \sum_{\ell=1}^N R_{k\ell} i_\ell(x, t) \\ &\quad - \sum_{\ell=1}^N L_{k\ell} \frac{\partial i_\ell(x, t)}{\partial t}, \\ k &= 1, \dots, N, 0 < x < D \end{aligned} \quad (1)$$

$$\begin{aligned} \frac{\partial i_k(x, t)}{\partial x} &= - \sum_{\ell=1}^N G_{k\ell} v_\ell(x, t) \\ &\quad - \sum_{\ell=1}^N B_{k\ell} \frac{\partial v_\ell(x, t)}{\partial t}, \\ k &= 1, \dots, N, 0 < x < D. \end{aligned} \quad (2)$$

In these equations, the self- (R_{kk}) and mutual ($R_{k\ell}$, $k \neq \ell$) resistances are due to conductor losses, the self- (L_{kk}) and mutual ($L_{k\ell}$, $k \neq \ell$) inductances determine the induced EMF due to the electromagnetic induction, the self- (G_{kk}) and mutual ($G_{k\ell}$, $k \neq \ell$) conductances are due to losses in the dielectrics, and the self- (B_{kk}) and mutual ($B_{k\ell}$, $k \neq \ell$) coefficients of electrostatic induction are due to the electrostatic effects. It is worth noting that (1) and (2) are valid only for a line with parameters which do not depend on frequency. If this is not the case, the line has to be described

by more complicated equations, which are beyond the scope of this paper.

Equations (1) and (2) can be put in a simpler form if we introduce the voltage and current vectors

$$[v(x, t)]_{N \times 1} = [v_1(x, t), \dots, v_N(x, t)]^T, \quad 0 < x < D \quad (3)$$

$$[i(x, t)]_{N \times 1} = [i_1(x, t), \dots, i_N(x, t)]^T, \quad 0 < x < D \quad (4)$$

where the superscript " T " denotes the transpose. Now we have instead of (1) and (2) the following matrix equations:

$$\frac{\partial [v(x, t)]}{\partial x} = -[R][i(x, t)] - [L] \frac{\partial [i(x, t)]}{\partial t} \quad (5)$$

$$\frac{\partial [i(x, t)]}{\partial x} = -[G][v(x, t)] - [B] \frac{\partial [v(x, t)]}{\partial t}. \quad (6)$$

These equations can be transformed into the frequency domain to read

$$\frac{d[V(x)]}{dx} = -[R][I(x)] - j\omega[L][I(x)], \quad 0 < x < D \quad (7)$$

$$\frac{d[I(x)]}{dx} = -[G][V(x)] - j\omega[B][V(x)], \quad 0 < x < D. \quad (8)$$

Here ω is the angular frequency, $[V(x)]$ is the vector of complex line voltages, and $[I(x)]$ is the vector of complex line currents. If we introduce the matrices of line impedances and admittances per unit length

$$[Z] = [R] + j\omega[L] \quad (9)$$

$$[Y] = [G] + j\omega[B] \quad (10)$$

(7) and (8) can be simplified to

$$\frac{d[V(x)]}{dx} = -[Z][I(x)], \quad 0 < x < D \quad (11)$$

$$\frac{d[I(x)]}{dx} = -[Y][V(x)], \quad 0 < x < D. \quad (12)$$

Note that (9) and (10) allow the elements of matrices $[R]$ and $[G]$, as well as those of matrices $[L]$ and $[B]$, to vary with frequency. However, in that case, going back to the time domain, we do not obtain (1) and (2) from (11) and (12), as noted before.

The telegrapher equations (5) and (6) in the time domain, or (11) and (12) in the frequency domain, fully describe the transmission line. However, in order to find the response of the line terminated by certain networks, one has to consider the telegrapher equations simultaneously with the equations describing the terminal networks. The latter equations represent boundary conditions for the telegrapher equations, at $x = 0$ and $x = D$. These equations give relationships between $[v(0, t)]$ and $[i(0, t)]$, at $x = 0$, and between $[v(D, t)]$ and $[i(D, t)]$, at $x = D$. There is no general form of these equations, since they depend on the terminal networks.

We are going to consider several special cases of linear terminal networks. The analysis of lines with nonlinear networks is postponed to Section VI. If the terminal networks consist of independent generators and linear, time-invariant resistors, the line voltages and currents satisfy the following boundary conditions:

$$[v(0, t)] = [v_C(t)] - [R_C][i(0, t)] \quad (13)$$

$$[v(D, t)] = [v_L(t)] + [R_L][i(D, t)]. \quad (14)$$

Here $[R_G]$ is the resistance matrix of the generator network, $[R_L]$ is the resistance matrix of the load network, $[v_G(t)]$ is the open-circuit voltage vector of the generator network, and $[v_L(t)]$ is the open circuit voltage vector of the load network. (For the sake of generality, we have assumed that generators can be present at both line ends, which are only arbitrarily referred to as the generator and load ends.)

Boundary conditions similar to (13) and (14) can be written in the frequency domain for more complex terminal networks, consisting of arbitrarily interconnected linear elements (e.g., resistors, capacitors, and inductors) and generators. In that case we have

$$[V(0)] = [V_G] - [Z_G][I(0)] \quad (15)$$

$$[V(D)] = [V_L] + [Z_L][I(D)] \quad (16)$$

where $[V_G]$ and $[V_L]$ are the complex open-circuit voltage vectors of the two-terminal networks, and $[Z_G]$ and $[Z_L]$ are the impedance matrices of these networks.

Note that in the above examples we have assumed that the terminal networks are mutually coupled only through the transmission line, i.e., we have assumed that there is no other circuit element connecting the two terminal networks.

Besides the boundary conditions, for the time-domain analysis we need to know a set of initial conditions for the line voltages and currents at a certain time instant t . In the present analysis we are going to assume that at $t = 0$ the line is empty, i.e., devoid of any voltages and currents. In other words, our initial conditions read

$$[v(x, 0)] = 0, \quad 0 < x < D \quad (17)$$

$$[i(x, 0)] = 0, \quad 0 < x < D. \quad (18)$$

For the purpose of the modal analysis, we have to derive the wave equations from the telegrapher equations. Let us first consider (5) and (6), in the time domain. Using simple manipulations with these equations we can get the wave equations in the time domain

$$\begin{aligned} \frac{\partial^2[v(x, t)]}{\partial x^2} &= [R][G][v(x, t)] + \{[R][B] + [L][G]\} \frac{\partial[v(x, t)]}{\partial t} \\ &\quad + [L][B] \frac{\partial^2[v(x, t)]}{\partial t^2}, \quad 0 < x < D \end{aligned} \quad (19)$$

$$\begin{aligned} \frac{\partial^2[i(x, t)]}{\partial x^2} &= [G][R][i(x, t)] + \{[B][R] + [C][L]\} \frac{\partial[i(x, t)]}{\partial t} \\ &\quad + [B][L] \frac{\partial^2[i(x, t)]}{\partial t^2}, \quad 0 < x < D. \end{aligned} \quad (20)$$

From these equations we can directly write the wave equations in the time domain for a lossless line

$$\frac{\partial^2[v(x, t)]}{\partial x^2} = [L][B] \frac{\partial^2[v(x, t)]}{\partial t^2}, \quad 0 < x < D \quad (21)$$

$$\frac{\partial^2[i(x, t)]}{\partial x^2} = [B][L] \frac{\partial^2[i(x, t)]}{\partial t^2}, \quad 0 < x < D. \quad (22)$$

Although (19) and (20), or (21) and (22), appear to be two independent matrix equations for the line voltages and currents, respectively, they are not independent, because the voltages and currents are mutually related through the telegrapher equations (5) and (6).

Starting from the telegrapher equations (11) and (12), in

the frequency domain, we can derive the wave equations in the frequency domain for a lossy transmission line as

$$\frac{d^2[V(x)]}{dx^2} = [Z][Y][V(x)], \quad 0 < x < D \quad (23)$$

$$\frac{d^2[I(x)]}{dx^2} = [Y][Z][I(x)], \quad 0 < x < D. \quad (24)$$

The following four sections are devoted to various procedures for solving the telegrapher and the wave equations, subject to appropriate boundary and initial conditions. Numerical examples are given in Section VII.

III. TIME-STEPPING SOLUTION

This method, sometimes also referred to as marching on in time, consists of making a finite-difference approximation to the partial derivatives in (5) and (6). The discretization with respect to the space coordinate (x) can be equivalent to an approximation of the transmission line by a lumped-element network. An example of such a network is shown in Fig. 2 for a three-conductor transmission line (i.e., $N = 2$). In this case, each signal conductor is replaced by a chain of T -networks. The mutual couplings between the conductors have been taken into account through the inductive, resistive, capacitive, and conductive coupling elements. Each cell approximates a transmission line section of length Δx . Hence, each inductive lumped element of the cell is given by $L_k/2 = (L_{kk}\Delta x)/2$, while mutual inductances are $L_{mkt}/2 = (L_{kt}\Delta x)/2$ ($k \neq t$). Since the inductive elements of two adjacent cells are connected in series, they can be replaced by a single element of inductance $L_{kk}\Delta x$. However, this procedure cannot be applied to the inductance elements located at the ends of the line. Similarly, each resistive element of the cell is given by $R_k/2 = (R_{kk}\Delta x)/2$, and mutual resistances are $R_{mkt}/2 = (R_{kt}\Delta x)/2$ ($k \neq t$). Note that the mutual resistances are due to the finite conductivity of the ground conductor, as well as to the eddy current induced in one signal conductor due to the current in another signal conductor. The adjacent resistances can be combined into a single resistance, just like the inductances. The capacitance of lumped elements connected between the signal conductors and ground are

$$C_k = \sum_{t=1}^N B_{kt}\Delta x$$

while the capacitances of the elements connected between the signal conductors are $C_{mkt} = -B_{kt}\Delta x$ ($k \neq t$). Similarly, conductances are given by

$$G_k = \sum_{t=1}^N G_{kt}\Delta x \quad \text{and} \quad G_{mkt} = -G_{kt}\Delta x \quad (k \neq t).$$

It should be pointed out that instead of the T -cells we could have utilized π -cells or half-cells in making the lumped-circuit equivalent of the transmission line. If the cell lengths are small enough, then, of course, the various models would yield similar results.

By approximating the transmission line by a network of T -cells, we have eliminated the derivatives with respect to space and replaced them by finite differences. Observe in this procedure that the voltage and current nodes are separated by a distance of $\Delta x/2$. This is in contrast to the classical methods for solving partial differential equations

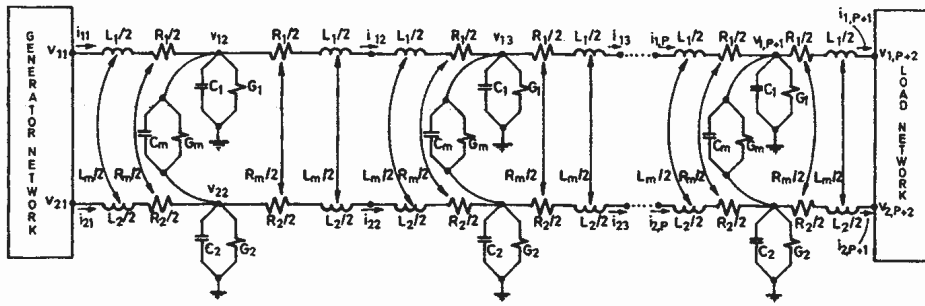


Fig. 2. Lumped-element equivalent circuit of a lossy transmission line with two signal conductors.

where the samples of both voltages and currents are taken at the same points along the x -axis.

For the network shown in Fig. 2 we now have

$$\begin{aligned}[v_{m+1}(t)] - [v_m(t)] &= -\alpha \Delta x [R] [i_m(t)] \\ &\quad - \alpha \Delta x [L] \frac{d[i_m(t)]}{dt}, \\ m &= 1, \dots, P+1 \end{aligned} \quad (25)$$

$$\begin{aligned}[i_{m+1}(t)] - [i_m(t)] &= -\Delta x [G] [v_{m+1}(t)] \\ &\quad - \Delta x [C] \frac{d[v_{m+1}(t)]}{dt}, \\ m &= 1, \dots, P. \end{aligned} \quad (26)$$

Here P is the number of cells, so that

$$\Delta x = D/P. \quad (27)$$

Also,

$$\begin{aligned}\alpha &= 1/2, \quad \text{for } m = 1 \text{ and } (P+1), \\ \text{and } \alpha &= 1, \quad \text{otherwise.} \end{aligned} \quad (28)$$

The vector $[v_m(t)]$ contains line voltages in the middle of the m th cell, except for $[v_1(t)]$ and $[v_{P+2}(t)]$ which contain line voltages at the generator and load ends, respectively. The vector $[i_m(t)]$ contains line current at the junction of the $(m-1)$ th and m th cells. Note that the positions at which the voltages $[v_m(t)]$ are defined are given by

$$\begin{aligned}x &= 0, \quad \text{for } m = 1, \quad x = D, \quad \text{for } m = P+2, \\ \text{and } x &= (m-3/2)\Delta x, \quad \text{otherwise.} \end{aligned} \quad (29)$$

The locations of the currents $[i_m(t)]$ are

$$x = (m-1)\Delta x, \quad m = 1, \dots, P+1. \quad (30)$$

Now we replace the time derivatives in (25) and (26) by the following finite-difference scheme:

$$\left. \frac{d[v_m(t)]}{dt} \right|_{t=n\Delta t} \approx \frac{[v_m(n+1)] - [v_m(n)]}{\Delta t} \quad (31)$$

$$\left. \frac{d[i_m(t)]}{dt} \right|_{t=n\Delta t} \approx \frac{[i_m(n+1)] - [i_m(n)]}{\Delta t} \quad (32)$$

where Δt is a prefixed time step. It is implied in (31) and (32) that $[v_m(n)]$ represents $[v_m(n\Delta t)]$ and $[i_m(n)]$ represents $[i_m(n\Delta t)]$. Substitution of (31) and (32) into (25) and (26) yields

$$\begin{aligned}[v_m(n+1)] &= \{[U] - \Delta t [B]^{-1} [G]\} [v_m(n)] \\ &\quad + \frac{\Delta t}{\Delta x} [B]^{-1} \{[i_{m-1}(n)] - [i_m(n)]\}, \\ m &= 2, \dots, P+1 \end{aligned} \quad (33)$$

$$\begin{aligned}[i_m(n+1)] &= \{[U] - \Delta t [L]^{-1} [R]\} [i_m(n)] \\ &\quad + \frac{\Delta t}{\Delta x} \frac{1}{\alpha} [L]^{-1} \{[v_m(n)] - [v_{m+1}(n)]\}, \\ m &= 1, \dots, P+1 \end{aligned} \quad (34)$$

where $[U]$ is the identity matrix.

Now, we solve the difference equations (33) and (34), subject to the boundary and initial conditions. If the terminal networks consist of generators and linear, time-invariant resistances, the boundary conditions (13) and (14) are valid, and they become

$$[v_1(n)] = [v_G(n)] - [R_G] [i_1(n)] \quad (35)$$

$$[v_{P+2}(n)] = [v_L(n)] + [R_L] [i_{P+1}(n)]. \quad (36)$$

The initial conditions are

$$[v_m(0)] = [0], \quad m = 2, \dots, P+1 \quad (37)$$

$$[i_m(0)] = [0], \quad m = 1, \dots, P+1 \quad (38)$$

where $[0]$ is a null vector.

The system of equations (33) and (34) along with the boundary conditions (35) and (36), and with the initial conditions (37) and (38) can be solved numerically by stepping in time, i.e., by successively taking $n = 1, 2, \dots$. Note that $[v_1(n)]$ and $[v_{P+2}(n)]$ should be determined from (35) and (36) prior to calculating $[i_m(n+1)]$ from (34).

The above procedure is equivalent to using Euler's method for solving a system of simultaneous differential equations.

The time-stepping procedure has certain advantages and drawbacks when compared to other methods. It is simple to code, but it takes a lot of computer time to execute. It can easily be interfaced to time-stepping procedures for solving terminal networks in the general case (i.e., nonlinear networks with memory). However, this procedure cannot be used for analysis of lines with frequency-dependent parameters, unless complicated equivalent networks are used for each conductor.

In the implementation of the time-stepping procedure care should be exercised to choose correctly the number of cells and the time step. The number of cells should be such that the line transit time over one cell is much shorter

than the rise (or fall) time of the waveforms considered (e.g., 10 times smaller). Too many cells greatly increase the running time. The time step should be much smaller than the transit time along a cell, in order to reduce parasitic oscillations and avoid divergence of the response. Numerical experiments have shown that the time step should be kept below about 1/20 of the transit time along a cell, at least for P in the range from 5 to 50. Of course, the stability of the time-stepping method can be improved by using more sophisticated methods for solving differential equations, rather than the Euler method, but in that case the simplicity of the programming, which might be the greatest advantage of the time-stepping method over the modal analysis, is definitely lost.

Numerical experiments have also shown that to obtain a good response a large number of cells is usually needed, which, in turn, requires a very small time step. Hence, the computer running time becomes prohibitively large if a good response is expected for a long transmission line, i.e., a line the transit time of which is much greater than the rise and fall times of the waveforms being transmitted along the line. A numerical example of the time-stepping solution is given in Section VII.

IV. MODAL ANALYSIS IN THE TIME DOMAIN

In this section we are going to consider only lossless lines. By force of the quasi-TEM approximation such lines have frequency-independent $[L]$ and $[B]$ matrices. A lossless line embedded in an inhomogeneous dielectric (the properties of which vary only over the line cross section, but not along the line length) is a dispersive transmission medium. However, there exist special sets of conductor voltages and currents for which the propagation is nondispersive. These sets are called the eigenmodes. (Generally, such modes in the time domain do not exist for lossy lines.) The line voltages and currents of an eigenmode can be represented as

$$[v^m(x, t)] = [V_0^m] g^m(t \mp x/c_m), \quad m = 1, \dots, N \quad (39)$$

$$[i^m(x, t)] = \pm [I_0^m] g^m(t \mp x/c_m), \quad m = 1, \dots, N \quad (40)$$

where the superscript "m" represents the m th eigenmode, c_m is the velocity of the m th eigenmode propagation along the transmission line, $[V_0^m]$ and $[I_0^m]$ are two sets of constants representing relative amplitudes of the conductor voltages and currents, and $g^m(t)$ is an arbitrary function of time, which we shall refer to as the mode intensity. The upper signs in the above equations correspond to an eigenmode traveling from the generator towards the load end, i.e., in the direction of the + x -axis. This eigenmode is usually referred to as the incident wave. The lower signs correspond to an eigenmode traveling in the opposite direction, and it is referred to as the reflected wave.

For a transmission line with N signal conductors there exist, in the general case, N linearly dependent vectors $[V_0^m]$ and corresponding $[I_0^m]$, which are unique to within a multiplicative constant, i.e., there exist N distinct eigenmodes. Each mode has its own velocity of propagation. However, in certain cases these velocities can coincide (e.g., if the line dielectric is homogeneous), and the modal voltage and current vectors are not linearly independent.

Note that $[V_0^m]$ and $[I_0^m]$ are related through (5) and (6), in which we have to put $[R] = [0]$ and $[G] = [0]$. Also, (39) and

(40) represent a particular solution to the wave equations (21) and (22).

If (39) is substituted into (21) we obtain

$$\left\{ \frac{1}{c_m^2} [U] - [L][B] \right\} [V_0^m] g^m(t \mp x/c_m) = 0 \quad (41)$$

where $[U]$ is the identity matrix. In order that (41) has non-trivial solutions for the line voltages, the determinant of the first term must be zero, i.e.,

$$\det \left\{ \frac{1}{c_m^2} [U] - [L][B] \right\} = 0. \quad (42)$$

Equation (42) is an eigenvalue equation, and $1/c_m^2$ is an eigenvalue of the matrix $[L][B]$. Therefore, we can consider $[V_0^m]$ to be an eigenvector of the matrix $[L][B]$ corresponding to the eigenvalue $1/c_m^2$. Since $[L][B]$ is an $N \times N$ matrix, there will be N eigenvalues (not necessarily distinct) and N eigenvectors. These eigenvalues and eigenvectors can be computed by using standard procedures (e.g., [30]).

Equation (22) can be transformed similarly to an eigenvalue equation through the substitution of (40), to yield

$$\det \left\{ \frac{1}{c_m^2} [U] - [B][L] \right\} = 0. \quad (43)$$

In this case, we would find $[I_0^m]$, which is an eigenvector of the matrix $[B][L]$ corresponding to the eigenvalue $1/c_m^2$. Note that the eigenvalues of the matrices $[L][B]$ and $[B][L]$ coincide, but the eigenvectors are, generally, different. As noted before, the voltage and current eigenvectors are related through (5) and (6). Hence

$$[I_0^m] = [L]^{-1} [V_0^m] \frac{1}{c_m} \quad (44)$$

$$[V_0^m] = [B]^{-1} [I_0^m] \frac{1}{c_m}. \quad (45)$$

At this point is it convenient to introduce two square matrices, $[S_V]$ and $[S_I]$, both of dimensions $N \times N$. The columns of these matrices are the voltage and current eigenvectors, respectively, i.e.,

$$[S_V] = \{[V_1], \dots, [V_N]\} \quad (46)$$

$$[S_I] = \{[I_1], \dots, [I_N]\}. \quad (47)$$

From (44)–(47) it follows that

$$[S_I] = [L]^{-1} [S_V] [\Lambda] \quad (48)$$

$$[S_V] = [B]^{-1} [S_I] [\Lambda] \quad (49)$$

where $[\Lambda]$ is a diagonal matrix the elements of which are $1/c_m$, $m = 1, \dots, N$, i.e.,

$$[\Lambda] = \text{diag} [1/c_1, \dots, 1/c_N]. \quad (50)$$

The conductor voltages and currents can be represented as sums of the incident and reflected waves in terms of the matrices $[S_V]$ and $[S_I]$. Hence

$$\begin{aligned} [v(x, t)] &= [v_{\text{inc}}(x, t)] + [v_{\text{ref}}(x, t)] \\ &= [S_V] \{[g_{\text{inc}}(x, t)] + [g_{\text{ref}}(x, t)]\} \end{aligned} \quad (51)$$

$$\begin{aligned} [i(x, t)] &= [i_{\text{inc}}(x, t)] + [i_{\text{ref}}(x, t)] \\ &= [S_I] \{[g_{\text{inc}}(x, t)] - [g_{\text{ref}}(x, t)]\} \end{aligned} \quad (52)$$

where

$$[g_{\text{inc}}(x, t)] = [g_{\text{inc}}^1(t - x/c_1), \dots, g_{\text{inc}}^N(t - x/c_N)]^T \quad (53)$$

$$[g_{\text{ref}}(x, t)] = [g_{\text{ref}}^1(t + x/c_1), \dots, g_{\text{ref}}^N(t + x/c_N)]^T. \quad (54)$$

The characteristic impedance matrix $[Z_c]$ of the transmission line is defined by the relations

$$[v_{\text{inc}}(x, t)] = [Z_c][i_{\text{inc}}(x, t)] \quad (55)$$

$$[v_{\text{ref}}(x, t)] = -[Z_c][i_{\text{ref}}(x, t)] \quad (56)$$

which must be valid for any incident and reflected wave, respectively. The characteristic admittance matrix $[Y_c]$ of the line is simply

$$[Y_c] = [Z_c]^{-1}. \quad (57)$$

Clearly, due to (51) and (52), the characteristic impedance matrix must satisfy the equation

$$[S_V] = [Z_c][S]. \quad (58)$$

Now from (48) and (49) we have

$$\begin{aligned} [Z_c] &= [S_V][S]^{-1} \\ &= [S_V][\Lambda]^{-1}[S_V]^{-1}[L] \\ &= [B]^{-1}[S_L][A][S]^{-1}. \end{aligned} \quad (59)$$

Our next concern will be the treatment of the terminal networks. There are two ways to simultaneously analyze the transmission line and the terminal networks. One way is to incorporate the analysis of the terminal networks into the analysis of the transmission line. For that purpose we have to know, at each time instant, the equivalent parameters of the terminal networks, as seen from the transmission line. These parameters can be, for example, the instantaneous Z-parameters of the terminal networks. The other way is to incorporate the analysis of the transmission line into the analysis of the terminal networks. For that purpose we have to know the instantaneous parameters of the transmission line, as seen from the two terminal networks.

Let us now consider the first approach. Suppose that we know the equivalent Thevenin's representation of the terminal networks, i.e., the resistance matrices $[R_C]$ and $[R_L]$, and the open-circuit voltage vectors $[v_C(t)]$ and $[v_L(t)]$. Note that we can allow the resistance matrices to be time-dependent. Such equivalent instantaneous parameters can be defined not only for purely resistive linear networks, which may contain generators, but also for any kind of linear networks, even with memory.

Combining (13) and (14) with the first parts of (51) and (52), and with (55) and (56), we obtain the following relations:

$$[v_{\text{inc}}(0, t)] = [\tau_C][v_C(t)] + [\rho_C][v_{\text{ref}}(0, t)] \quad (60)$$

$$[v_{\text{ref}}(D, t)] = [\tau_L][v_L(t)] + [\rho_L][v_{\text{inc}}(D, t)]. \quad (61)$$

Here $[\tau_C]$, $[\rho_C]$, $[\tau_L]$, and $[\rho_L]$ are called the generator transmission coefficient, generator reflection coefficient, load transmission coefficient, and load reflection coefficient, respectively. All four matrices have the same dimensions, $N \times N$. These matrices are given by

$$[\tau_C] = [Z_c]\{[R_C] + [Z_c]\}^{-1} \quad (62)$$

$$[\rho_C] = \{[R_C] - [Z_c]\}\{[R_C] + [Z_c]\}^{-1} \quad (63)$$

$$[\tau_L] = [Z_c]\{[R_L] + [Z_c]\}^{-1} \quad (64)$$

$$[\rho_L] = \{[R_L] - [Z_c]\}\{[R_L] + [Z_c]\}^{-1}. \quad (65)$$

The voltages $[v_{\text{inc}}(x, t)]$ and $[v_{\text{ref}}(x, t)]$ can be related to the modal intensities $[g_{\text{inc}}(x, t)]$ and $[g_{\text{ref}}(x, t)]$, respectively, by using (51) and (52). Thus we get

$$[g_{\text{inc}}(0, t)] = [\tau_C^m][v_C(t)] + [\rho_C^m][g_{\text{ref}}(0, t)] \quad (66)$$

$$[g_{\text{ref}}(D, t)] = [\tau_L^m][v_L(t)] + [\rho_L^m][g_{\text{inc}}(D, t)]. \quad (67)$$

We shall refer to the $N \times N$ matrices $[\tau_C^m]$, $[\rho_C^m]$, $[\tau_L^m]$, and $[\rho_L^m]$ as the modal transmission and reflection coefficients. These $N \times N$ matrices are defined by

$$[\tau_C^m] = [S_V]^{-1}[\tau_C] \quad (68)$$

$$[\rho_C^m] = [S_V]^{-1}[\rho_C][S_V] \quad (69)$$

$$[\tau_L^m] = [S_V]^{-1}[\tau_L] \quad (70)$$

$$[\rho_L^m] = [S_V]^{-1}[\rho_L][S_V]. \quad (71)$$

The advantage of dealing with the modal transmission and reflection coefficient is that we can directly trace the individual modes, without having to find the conductor voltages and currents. However, the conductor voltages and currents can be calculated at any point if the modal waveforms are known by utilizing (51) and (52).

Assuming that the terminal network Z-parameters are known, we can now determine the modal intensities $[g_{\text{inc}}(x, t)]$ and $[g_{\text{ref}}(x, t)]$. If the terminal network parameters are given analytically, the modal intensities can be obtained by an analytical procedure. However, for each mode we have to track a wave being launched from one transmission line end, reaching the other line end, being reflected from that end, reaching the first end, being re-reflected from that end, etc. At each reflection each mode, generally, excites both that mode and all the other modes. After a few transitions along the line the analytical procedure might become pretty cumbersome and it might not be suitable for a computer implementation.

In the case when the analytical mode tracking is impractical, we can use only time samples of the modal intensities to obtain a computationally simple and efficient algorithm for mode tracking. For simplicity, let us suppose that we are sampling uniformly, with a sampling interval Δt . Let us also start at $t = 0$, assuming that the initial conditions (17) and (18) are valid. In that case, initially, the samples of $[g_{\text{inc}}(0, k\Delta t)]$ and $[g_{\text{ref}}(D, k\Delta t)]$, $k = 0, 1, \dots$, are readily available, because we know the open-circuit voltage vectors $[v_C(k\Delta t)]$ and $[v_L(k\Delta t)]$. (We assume that generators can exist at both line ends.) At that early time, the incident wave has not yet reached the load end, nor has the reflected wave reached the generator end. However, after one line transit time, defined for each mode as D/c_m , the incident and the reflected waves appear at the load end and at the generator end, respectively. The samples of these waves are already known, because the intensities of these waves are exactly the same as at the line end from which the waves have been launched, but they are only delayed in time by D/c_m . Hence, the samples of the waves launched from the line ends are again easily calculated from (66) and (67). For such a case we can easily track the modes after as long a time interval as we wish. It suffices to store the samples of $[g_{\text{inc}}(0, t)]$ and $[g_{\text{ref}}(D, t)]$ in appropriate shift registers, and compute conductor voltages and/or currents at both line ends. The length of the registers (i.e., the number of samples S kept in these

registers) must be such that the time interval spanned by the samples ($S\Delta t$) is longer than the longest modal transit time from one transmission line end to the other, i.e.,

$$S\Delta t > \max_m \{D/c_m\}. \quad (72)$$

The only problem in such a mode tracking method is that generally D/c_m , $m = 1, \dots, N$, is not an integral multiple of Δt . Hence, the samples $[g_{inc}(D, k\Delta t)]$ cannot be obtained directly from the samples $[g_{inc}(0, k\Delta t)]$, by simply delaying the latter samples. A similar conclusion is valid for obtaining the samples $[g_{ref}(0, k\Delta t)]$ from $[g_{ref}(D, k\Delta t)]$. However, an interpolation between the samples can be applied. For example, if we take a linear interpolation, for t in the interval

$$k\Delta t < t < (k+1)\Delta t \quad (73)$$

we obtain

$$\begin{aligned} g_{inc}^m(0, t) &= \frac{t - k\Delta t}{\Delta t} g_{inc}^m(0, (k+1)\Delta t) \\ &\quad - \frac{t - (k+1)\Delta t}{\Delta t} g_{inc}^m(0, k\Delta t) \end{aligned} \quad (74)$$

$$\begin{aligned} g_{ref}^m(D, t) &= \frac{t - k\Delta t}{\Delta t} g_{ref}^m(D, (k+1)\Delta t) \\ &\quad - \frac{t - (k+1)\Delta t}{\Delta t} g_{ref}^m(D, k\Delta t). \end{aligned} \quad (75)$$

Equations (74) and (75) enable us to determine the interpolated values of the launched waves which we need to obtain the propagated waves at the other end (delayed, of course, by D/c_m).

The above procedure cannot be applied if the terminal networks are nonlinear, because for such networks we cannot obtain a linear Thévenin equivalent (i.e., the instantaneous Z-parameters). In such cases, we have to use a special program for solution of the terminal networks and incorporate the analysis of the transmission line into the analysis of the terminal networks. Thereby we need to have instantaneous Z-parameters of the transmission line, as seen by the terminal networks. It can be proved easily that a lossless transmission line can equivalently be represented with respect to its terminals by two networks, each of the networks corresponding to one line end. The networks are purely resistive, with time-independent resistances, and the resistance matrices of the networks are identical to the characteristic impedance matrix of the transmission line. Ideal voltage generators, the EMFs of which equal twice the voltage of the wave incoming on that port, are connected in series with this resistive network. This equivalent representation is sketched in Fig. 3. The terminal networks have

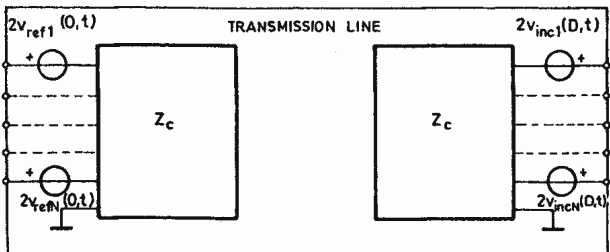


Fig. 3. Equivalent Thévenin representation of a lossless transmission line.

to be analyzed in the time domain (which is practically the only possibility for nonlinear networks), by some kind of a marching-on-in-time procedure. The transmission-line model can easily be incorporated into such an analysis because now, at each time step, we have the equivalent representation of the line. Note that the EMFs of the equivalent network are known, because they are given in terms of the delayed modal intensities launched from the opposite line ends (delayed by D/c_m). In order to prepare data for further time steps, we have to find (and store) the waveforms launched from the line ends. Thus the voltage wave launched from the generator towards the load end is given by

$$[v_{inc}(0, t)] = [v(0, t)] - [v_{ref}(0, t)] \quad (76)$$

while the voltage wave launched from the load towards the generator end is given by

$$[v_{ref}(D, t)] = [v(D, t)] - [v_{inc}(D, t)]. \quad (77)$$

Note that in the above equations $[v_{ref}(0, t)]$ and $[v_{inc}(D, t)]$ are known, while $[v(0, t)]$ and $[v(D, t)]$ are supplied by the procedure for solving the generator, and the load network, and they correspond to the current time sample. Knowing $[v_{inc}(0, t)]$ and $[v_{ref}(D, t)]$, we can find $[g_{inc}(0, t)]$ and $[g_{ref}(0, t)]$ from (51) and track the modes to the other line end.

The solution of nonlinear networks without memory is reduced to solving, at each time step, a set of simultaneous nonlinear equations, which can be accomplished by using certain iterative techniques (e.g., the Newton-Raphson method, or optimization methods). The solution of nonlinear networks with memory is based on solving nonlinear differential equations, which can, again, be done in a variety of ways. Perhaps the simplest, but least accurate, technique is the Euler method.

Some numerical examples of modal analysis in the time domain are given in Section VII.

V. MODAL ANALYSIS IN THE FREQUENCY DOMAIN

We can use modal analysis in the frequency domain for an arbitrary transmission line, including lines with losses and frequency-dependent $[L]$, $[R]$, $[B]$, and $[G]$ matrices. However, the terminal networks have to be linear and time-invariant. Regarding the time-domain excitations contained in these networks, we have to find the Fourier transform of their waveforms (usually by applying the fast Fourier transform) to obtain the complex amplitudes of the waveforms in the frequency domain, at a set of discrete frequencies. Each of these individual frequency components is then considered to excite the transmission line. The modal analysis is performed at each frequency, and thereby we obtain the frequency response of the transmission line at both the generator and load ends. The inverse fast Fourier transform is then applied to these frequency responses to find the time-domain response.

Let us consider the transmission line in the frequency domain. We can assume that the eigenmodes propagate along the line in a form given by $\exp(\mp \gamma_m x)$, where γ_m is the propagation coefficient for the m th eigenmode. Again, the “-” sign in the exponent corresponds to the incident wave, and “+” to the reflected wave. Note that for a lossless transmission line γ_m is purely imaginary (and equal to $j\omega/c_m$), while for a lossy line it has both real and imaginary

parts. Therefore, instead of (39) and (40) we now have the phasor representations for the modal voltages and currents

$$[V^m(x)] = [V_0^m] \exp(\mp \gamma_m x) \quad (78)$$

$$[I^m(x)] = \pm [I_0^m] \exp(\mp \gamma_m x) \quad (79)$$

where $[V_0^m]$ and $[I_0^m]$ are complex vectors of constants.

If we substitute (78) and (79) into (11) and (12), we obtain

$$\mp \gamma_m [V_m(x)] = -[Z][I_m(x)] \quad (80)$$

$$\mp \gamma_m [I_m(x)] = -[Y][V_m(x)] \quad (81)$$

and from the wave equations (23) and (24) we obtain

$$\{\gamma_m^2[u] - [Z][Y]\}[V_0^m] \exp(\mp \gamma_m x) = 0 \quad (82)$$

$$\{\gamma_m^2[u] - [Y][Z]\}[I_0^m] \exp(\mp \gamma_m x) = 0. \quad (83)$$

Hence, the corresponding eigenvalue equations become

$$\det\{\gamma_m^2[u] - [Z][Y]\} = 0 \quad (84)$$

$$\det\{\gamma_m^2[u] - [Y][Z]\} = 0. \quad (85)$$

From either of the equations the complex eigenvalues γ_m^2 can be computed, together with one of the complex eigenvectors $[V_0^m]$ or $[I_0^m]$. As before, if we define the matrix $[S_V]$ as the matrix containing the complex eigenvectors of the voltages and $[S_I]$ as the matrix containing the complex eigenvectors of the current, they will now be related by

$$[S_I] = [Z]^{-1}[S_V][\Gamma] \quad (86)$$

where

$$[\Gamma] = \text{diag}\{\gamma_1, \dots, \gamma_N\}. \quad (87)$$

The matrices $[S_V]$ and $[S_I]$ are defined by (46) and (47), respectively. Instead of the vectors $[g_{\text{inc}}(x, t)]$ and $[g_{\text{ref}}(x, t)]$, defined for the modal analysis in the time domain, we now introduce the complex vectors

$$[G_{\text{inc}}(x)] = [G_{\text{inc}}^1 \exp(-\gamma_1 x), \dots, G_{\text{inc}}^N \exp(-\gamma_N x)]^T \quad (88)$$

$$[G_{\text{ref}}(x)] = [G_{\text{ref}}^1 \exp(\gamma_1 x), \dots, G_{\text{ref}}^N \exp(\gamma_N x)]^T \quad (89)$$

where $G_{\text{inc}}^1, \dots, G_{\text{inc}}^N$ and $G_{\text{ref}}^1, \dots, G_{\text{ref}}^N$ are complex constants. The characteristic impedance of the line can now be found as

$$\begin{aligned} [Z_c] &= [S_V][S_I]^{-1} \\ &= [S_V][\Gamma]^{-1}[S_V]^{-1}[Z] \\ &= [Y]^{-1}[S_I][\Gamma][S_I]^{-1}. \end{aligned} \quad (90)$$

Assuming that the terminal networks are characterized by their Z-parameters, (15) and (16), we obtain

$$[G_{\text{inc}}(0)] = [\tau_C^m][V_C] + [\rho_C^m][G_{\text{ref}}(0)] \quad (91)$$

$$[G_{\text{ref}}(D)] = [\tau_L^m][V_L] + [\rho_L^m][G_{\text{inc}}(D)] \quad (92)$$

where the modal reflection and transmission coefficients at the generator and load ends are given by

$$[\tau_C^m] = [S_V]^{-1}[\tau_C] \quad (93)$$

$$[\rho_C^m] = [S_V]^{-1}[\rho_C][S_V] \quad (94)$$

$$[\tau_L^m] = [S_V]^{-1}[\tau_L] \quad (95)$$

$$[\rho_L^m] = [S_V]^{-1}[\rho_L][S_V] \quad (96)$$

while the voltage transmission and reflection coefficients are

$$[\tau_C] = [Z_c]([Z_c] + [Z_L])^{-1} \quad (97)$$

$$[\rho_C] = ([Z_c] - [Z_L])([Z_c] + [Z_L])^{-1} \quad (98)$$

$$[\tau_L] = [Z_c]([Z_L] + [Z_c])^{-1} \quad (99)$$

$$[\rho_L] = ([Z_L] - [Z_c])([Z_L] + [Z_c])^{-1}. \quad (100)$$

The relations between the modal voltages at $x = 0$ and $x = D$ can now be written as

$$[G_{\text{inc}}(D)] = [E][G_{\text{inc}}(0)] \quad (101)$$

$$[G_{\text{ref}}(0)] = [E][G_{\text{ref}}(D)] \quad (102)$$

where $[E]$ is a diagonal matrix,

$$[E] = \text{diag}\{\exp(-\gamma_1 D), \dots, \exp(-\gamma_N D)\}. \quad (103)$$

Utilizing (101) and (102) in (91) and (92), we obtain

$$\begin{aligned} [G_{\text{inc}}(0)] &= [\tau_C^m][V_C] + [\rho_C^m][E][\rho_L^m][E][G_{\text{inc}}(0)] \\ &\quad + [\rho_L^m][E][\tau_L^m][V_L] \end{aligned} \quad (104)$$

$$[G_{\text{ref}}(D)] = [\tau_L^m][V_L] + [\rho_L^m][E][G_{\text{inc}}(0)] \quad (105)$$

whence $[G_{\text{inc}}(0)]$ and $[G_{\text{ref}}(D)]$ can easily be evaluated.

Special formulas must be used to compute the line response for zero frequency, because in certain cases one or both of the matrices $[Z]$ and $[Y]$ are zero, and the eigenvalues cannot be computed. If the line is lossless, i.e., if $[R] = [0]$ and $[G] = [0]$, we have

$$\begin{aligned} [V(0)] &= [V(D)] \\ &= [Z_c]([Z_c] + [Z_L])^{-1}[V_C] + [Z_c]([Z_c] + [Z_L])^{-1}[V_L] \end{aligned} \quad (106)$$

where now all the matrices are real. If $[R] \neq [0]$ and $[G] = 0$, then

$$[V(0)] = [V_C] - [Z_c]([Z_c] + [Z_L] + [R]D)^{-1}([V_C] - [V_L]) \quad (107)$$

$$\begin{aligned} [V(D)] &= [V_L] + [Z_L]([Z_c] + [Z_L] + [R]D)^{-1}([V_C] - [V_L]). \end{aligned} \quad (108)$$

When $[R] = [0]$ and $[G] \neq [0]$, then

$$\begin{aligned} [V(0)] &= [V(D)] \\ &= ([Z_c]^{-1} + [Z_L]^{-1} + [G]D)^{-1}([Z_c]^{-1}[V_C] + [Z_L]^{-1}[V_L]). \end{aligned} \quad (109)$$

Finally, if $[R] \neq [0]$ and $[G] \neq [0]$, modal analysis can be performed.

Knowing $[G_{\text{inc}}(0)]$ and $[G_{\text{ref}}(D)]$ it is easy to find the conductor voltages at the transmission line ends as

$$[V(0)] = [S_V]\{[G_{\text{inc}}(0)] + [E][G_{\text{ref}}(D)]\} \quad (110)$$

$$[V(D)] = [S_V]\{[E][G_{\text{inc}}(0)] + [G_{\text{ref}}(D)]\}. \quad (111)$$

Bearing in mind that we are using the fast Fourier transform to convert from the time domain to the frequency domain, and back, it is obvious that the voltage excitations in the time domain must have a sufficiently long trailing time interval where they are equal to zero. During this inter-

val, the transmission line response should practically settle to zero. The reason for ensuring this is because the application of the fast Fourier transform inherently introduces a periodical repetition of the waveforms. So, if the settling interval is not long enough, the responses would overlap, yielding incorrect results.

VI. NONLINEARLY LOADED TRANSMISSION LINES

As mentioned in the previous sections, the analysis of arbitrary nonlinear terminal networks (with or without memory), in the general case, can be performed only in the time domain. On the other hand, the analysis of lossy transmission lines (as well as lines with frequency-dependent parameters) should be performed in the frequency domain, as discussed in Section V. So, in order to combine the two cases, i.e., to design a method for analysis of lossy transmission lines with arbitrary nonlinear terminal networks, one must be able to combine the solutions in the two domains. Since the transmission line is a linear network, it can be completely characterized in the time domain by its Green's functions, which are, in turn, obtained from the frequency-domain analysis. These functions can be implemented in a time-domain solution of the terminal networks in a manner shown below.

Consider a linear, passive n -port network. Suppose that an ideal voltage generator, of EMF $v_{j0}(t)$, is connected at the port j , while the other ports are short-circuited. One can solve for the currents at the network ports. All these currents can be represented in the form

$$I_k(\omega) = Y_{kj}(\omega) V_{j0}(\omega), \quad k = 1, \dots, n \quad (112)$$

where $V_{j0}(\omega)$ is the Fourier transform of $v_{j0}(t)$ and $Y_{kj}(\omega)$ are the network Y -parameters. Let us suppose, for a moment, that $v_{j0}(t)$ is a unit delta function. In that case, $V_{j0}(\omega) = 1$, independently of frequency, and the currents in the time domain are obtained as

$$i_k(t) = i_{gkj}(t) = F^{-1}\{Y_{kj}(\omega)\} \quad (113)$$

where F^{-1} denotes the inverse Fourier transform. These currents are referred to as the network Green's functions. (There are two things to be noted. First, the reference direction for the generator EMF and the current at that port coincide, by convention. Second, if the network is reciprocal, as in our case, then $i_{gkj}(t) = i_{gjk}(t)$.)

For an arbitrary $v_{j0}(t)$ we have

$$i_k(t) = F^{-1}\{Y_{kj}(\omega) V_{j0}(\omega)\} = i_{gkj}(t) * v_{j0}(t) \quad (114)$$

where “*” denotes convolution. We now consider the same network driven by ideal voltage generators at all the ports. Hence, from superposition we can write

$$i_k(t) = \sum_{j=0}^n \int_0^t i_{gkj}(t-\theta) v_{j0}(\theta) d\theta. \quad (115)$$

In the convolution integral it is assumed that all excitations begin after $t = 0$. It should be noted that, by the compensation theorem, the ideal voltage generators driving the network can represent the (known) voltages at the network ports, irrespective of what is actually connected to the ports.

Following the above approach, we would have to connect an ideal delta-function generator between one of the transmission line conductors (at one line end) and ground, short-

circuit other line ports, perform modal analysis in the frequency domain to find the conductor currents, and compute their inverse Fourier transforms to obtain Green's functions. This should be repeated for all line conductors.

There are, however, several problems that should be considered. First, the analysis of the transmission line is usually done only numerically, at a finite number of discrete frequencies. In turn, in the time domain, Green's functions must also be discretized and of finite duration. Second, these Green's functions must be convolved with line port voltages, which must also be done numerically. The convolution turns out to be the most time-consuming part of the present analysis, and therefore the number of samples of Green's functions should be kept as low as possible. This can be a particular problem if the analysis of the response of the line with terminal networks is to span a time interval greater than a few line transit times. Namely, if the line ports are short-circuited (as they are for the computation of Green's functions), the line response exceeds many transit times in duration, even for a moderately lossy line. For a lossless line with short-circuited ports the response is of an infinite duration! Therefore, the line Green's functions would have to be kept in very long registers, spanning the same time interval as the time interval in which we would like to analyze the response of the transmission line terminated by arbitrary nonlinear networks. This is, of course, not only a computer-storage problem, but also demands very long execution times.

The lengths of the registers mentioned above can be kept relatively short if the duration of Green's functions can be reduced to only a few line transit times. However, this is possible only if the line is reasonably well matched. For example, if a lossless line is terminated by perfectly matched networks, the duration of the line response to a delta-function generator connected at one line port is only one sample for all the ports at the line end where that generator is connected, while the response at the ports at the other end of the line terminates after one line transit time. For lossy lines, with moderately low losses (as normally used in practice), the situation is very similar.

Following this example, we can artificially insert at every port (i.e., line conductor at the generator and load ends) a linear frequency-independent resistance so as to significantly reduce reflections from both line ends, as compared to the case where the ports are merely short-circuited. (A more general approach to this problem can be found in [31].) A good choice of these resistances is to take them equal to the corresponding diagonal elements of the line characteristic impedance matrix $[Z_c]$, i.e., Z_{ckk} , assuming the line to be lossless, i.e., by taking $[R] = [0]$ and $[G] = [0]$. The transmission line augmented by these resistances can be considered as a new n -port network (see Fig. 4), and its Green's functions can be computed as described above. Thereby, in practical cases of lossy lines, the line response (when computing Green's functions) is confined to about 3–6 line transit times, and Green's function registers have to cover only this time span.

However, by introducing these resistances, we have changed the line characteristics as seen by the terminal networks. To restore the original characteristics, we have to introduce in series with the terminal network ports negative resistances, equal to $-Z_{ckk}$, as shown in Fig. 4. Note that these resistances are frequency-independent, and thus

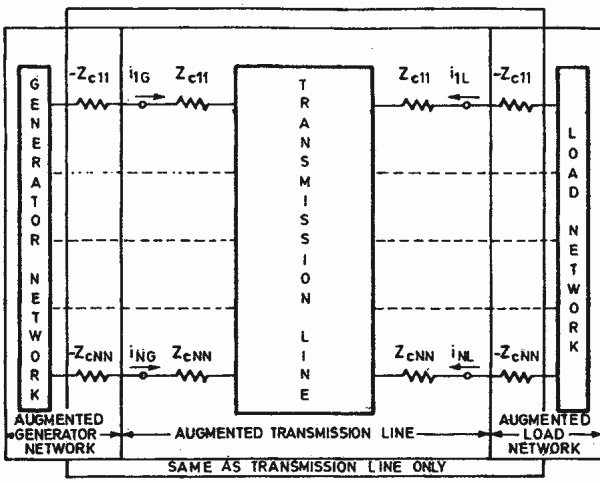


Fig. 4. Equivalent representation of a lossy transmission line with arbitrary terminal networks.

they do not complicate the time-domain analysis of the terminal networks.

Considering now the augmented transmission line (the line with Z_{ckk} resistors) as a network with $n = 2N$ ports, we can determine Green's functions. With these functions known, we can relate line conductor currents to the line port voltages $v_v(t)$ by using (115), where $v_{j0}(t)$ should be substituted by $v_{vj}(t)$. In order to distinguish between the line ports at the generator end and at the load end, we can rewrite (115) as

$$i_{kG}(t) = \sum_{j=1}^N \int_0^t i_{gkj}^s(t-\theta) v_{vjG}(\theta) d\theta + \sum_{j=1}^N \int_0^t i_{gkj}^m(t-\theta) v_{vjL}(\theta) d\theta, \quad k = 1, \dots, N \quad (116)$$

$$i_{kL}(t) = \sum_{j=1}^N \int_0^t i_{gkj}^m(t-\theta) v_{vjG}(\theta) d\theta + \sum_{j=1}^N \int_0^t i_{gkj}^s(t-\theta) v_{vjL}(\theta) d\theta, \quad k = 1, \dots, N. \quad (117)$$

In these equations, i_{gkj} is the Green's function representing the current in the conductor k when the delta-function generator drives the conductor j at the same line end, while i_{gkj}^m corresponds to the case when the current is computed at one line end, while the excitation is at the other end. Obviously, due to the symmetry of the transmission line, it is irrelevant which end of the line is taken as the first one and which as the second one.

If we now connect the terminal networks augmented by the negative resistances to the augmented transmission line (see Fig. 4), the conductor currents and the voltages between the junctions of Z_{ckk} and $-Z_{ckk}$ and the ground are related by (116) and (117). Note that the series combination of Z_{ckk} and $-Z_{ckk}$ essentially represents a mere short circuit, as it must be, because from both the transmission line and the terminal network sides we should see no change by introducing these fictitious resistances. For brevity, we shall refer to the voltages $v_v(t)$ as the virtual terminal voltages.

In order to prepare (116) and (117) for a computer imple-

mentation, we have to replace the integrations by summations. Thus we obtain

$$i_{kG}(q) = \sum_{j=1}^N \sum_{p=0}^q i_{gkj}^s(q-p) v_{vjG}(p) \Delta t + \sum_{j=1}^N \sum_{p=0}^q i_{gkj}^m(q-p) v_{vjL}(p) \Delta t, \quad k = 1, \dots, N \quad (118)$$

$$i_{kL}(q) = \sum_{j=1}^N \sum_{p=0}^q i_{gkj}^m(q-p) v_{vjG}(p) \Delta t + \sum_{j=1}^N \sum_{q=0}^N i_{gkj}^s(q-p) v_{vjL}(p) \Delta t, \quad k = 1, \dots, N \quad (119)$$

where the argument q denotes the time instant, $q\Delta t$, at which we sample the voltages and currents. We can modify the sums on the right-hand sides of (118) and (119) by extracting the terms for $p = q$. Noting that $i_{gkj}^s(0) \neq 0$, and $i_{gkj}^m(0) = 0$ (due to the line delay), we have

$$i_{kG}(q) = \sum_{j=1}^N i_{gkj}^s(0) v_{vjG}(q) \Delta t + \sum_{j=1}^N \sum_{p=0}^{q-1} i_{gkj}^s(q-p) v_{vjG}(p) \Delta t + \sum_{j=1}^N \sum_{p=0}^{q-1} i_{gkj}^m(q-p) v_{vjL}(p) \Delta t, \quad k = 1, \dots, N \quad (120)$$

$$i_{kL}(q) = \sum_{j=1}^N i_{gkj}^s(0) v_{vjL}(q) \Delta t + \sum_{j=1}^N \sum_{p=0}^{q-1} i_{gkj}^m(q-p) v_{vjG}(p) \Delta t + \sum_{j=1}^N \sum_{p=0}^{q-1} i_{gkj}^s(q-p) v_{vjL}(p) \Delta t, \quad k = 1, \dots, N. \quad (121)$$

Note that the first sum in either (120) or (121) contains virtual terminal voltages only for $t = q\Delta t$, i.e., at the same time instant for which the current on the left-hand side is computed, while the second (double) sum contains only previous values of the voltages, i.e., the history of the network. Noting that $i_{gkj}^s(0)$ are constants for a given transmission line, the first sum can be represented for $k = 1, \dots, N$ in the form $[G_{vd}] [v_v]$, where $[v_v]$ is a column matrix containing the virtual terminal voltages, and $[G_{vd}]$ is an $N \times N$ square matrix, the elements of which are $i_{gkj}^s(0)$. The matrix $[G_{vd}]$ can be considered as a conductance matrix giving the instantaneous (dynamic) input conductance to the transmission line, as seen from the virtual terminals. The double sum represents a current. It can be considered as the current of a current generator, the current of which does not depend on the instantaneous values of the transmission line currents and voltages, but rather only on their previous values. Again, if we consider $k = 1, \dots, N$, these independent currents can be represented by a column matrix $[i_c]$, where the subscript "c" points out that these currents are obtained by convolving the Green's functions and the virtual terminal voltages. Thus (120) and (121) can be written in a shorter form as

$$[i_G(q)] = [G_{vd}] [v_{vG}(q)] + [i_{cG}(q-1)] \quad (122)$$

$$[i_L(q)] = [G_{vd}] [v_{vL}(q)] + [i_{cL}(q-1)]. \quad (123)$$

We can now solve (122) and (123) for the virtual voltages at $t = q\Delta t$ to obtain

$$[v_{vc}(q)] = [G_{vd}]^{-1}[i_C(q)] - [G_{vd}]^{-1}[i_{cc}(q-1)] \quad (124)$$

$$[v_{vl}(q)] = [G_{vd}]^{-1}[i_L(q)] - [G_{vd}]^{-1}[i_{cl}(q-1)] \quad (125)$$

where $[i_C]$ and $[i_L]$ are column matrices containing terminal currents. The real (true) terminal voltages at the transmission line ports can be obtained as

$$\begin{aligned} [v_C(q)] &= [v_{vc}(q)] + \text{diag}(-Z_c)[i_C(q)] \\ &= [R_d][i_C(q)] - [G_{vd}]^{-1}[i_{cc}(q-1)] \end{aligned} \quad (126)$$

$$\begin{aligned} [v_L(q)] &= [v_{vl}(q)] + \text{diag}(-Z_c)[i_L(q)] \\ &= [R_d][i_L(q)] - [G_{vd}]^{-1}[i_{cl}(q-1)] \end{aligned} \quad (127)$$

where $\text{diag}(-Z_c)$ is a diagonal matrix the elements of which are $-Z_{ckk}$, and

$$[R_d] = [G_{vd}]^{-1} + \text{diag}(-Z_c) \quad (128)$$

is the dynamic input resistance matrix of the line, as seen from the terminal networks. The term $-[G_{vd}]^{-1}[i_C]$ can be considered as the line open-circuit voltage vector. Hence, we have managed to obtain the line equivalent instantaneous Z-parameters, as seen by the (nonaugmented) terminal networks. It is worth noting that the dynamic input resistance matrix is time constant. For a lossless line with frequency-independent parameters this matrix equals the characteristic impedance matrix.

Once we have determined the equivalent line Z-parameters in the time domain, our analysis becomes similar to the analysis of the response of a lossless line, described in Section IV. The only difference between the two cases is in the actual computation of the open-circuit voltage vectors: in Section IV they were computed by tracking the mode propagation in the time domain, while here they are evaluated by using the convolution. Therefore, everything regarding the way of combining the solutions of the transmission line and the terminal networks remains valid for lossy transmission lines, and shall not be repeated here.

VII. EXAMPLES

To illustrate the theory presented above, we here consider a few examples.

The first example is the transmission line consisting of two signal conductors and a ground plane, schematically represented in Fig. 5. The line is assumed to be 304.8 mm long, with $L_{11} = L_{22} = 494.6 \text{ nH/m}$, $L_{12} = L_{21} = 63.3 \text{ nH/m}$, $B_{11} = B_{22} = 62.8 \text{ pF/m}$, and $B_{12} = B_{21} = -4.94 \text{ pF/m}$. At one port, the line is excited by a voltage generator, of an internal

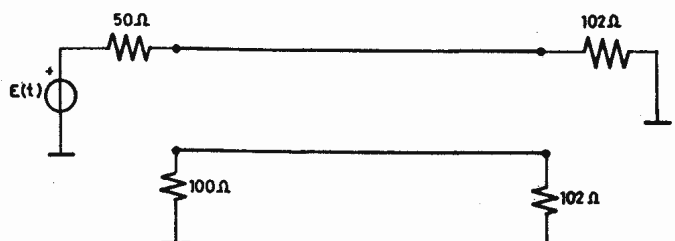


Fig. 5. Example of a transmission line with two signal conductors and linear resistive terminal networks, excited by a voltage generator.

impedance of 50Ω , the EMF of which is assumed to be a ramp, continued by a steady voltage, as shown in Fig. 6. This EMF approximates the leading edge of a pulse. The other conductor at the generator end is connected to the ground through a $100-\Omega$ resistor.

Let us first assume that the line is lossless, and that at the load end the conductors are connected to the ground through $102-\Omega$ resistors. The line response in this case is presented in Fig. 7, and it was obtained by the modal analysis in the time domain. The same case was also analyzed by the time-stepping technique, by utilizing 50 T-cells, and with a time step $\Delta t = 0.1 \text{ ps}$, and by the modal analysis in the frequency domain. In the latter case, 1024 samples were taken in the time domain, at a sampling frequency of 80 GHz. Since the fast Fourier transform deals with periodically repeated waveforms in the time domain, the excitation function had to be modified so as to return to zero after 6 ns. The interval at which this function was forced to be zero (i.e., from 6 to 12.8 ns) was chosen so that the line response settled down reasonably well before the next ramp started (at 12.8 ns). The line responses obtained by these two techniques differ appreciably from the results computed by using the modal analysis in the time domain only for the voltage at the load end of the parasitic (nondriven) conductor. They are shown in Fig. 8. Note the oscillations in the response obtained by the time-stepping solution (Fig. 8(a)). The ringing frequency is directly proportional to the number of cells utilized in the model. In the response obtained by modal analysis in the frequency domain (Fig. 8(b)) one can note tails of the preceding pulses, as well as small oscillations due to the finite bandwidth of the FFT.

Next we consider the same transmission line as above, but with losses, and terminated at the load end in two nonlinear networks, sketched in Fig. 9. The nonlinear resistor V/I characteristics was assumed to be of the form

$$I_n(V_n) = 10(e^{V_n/2V_t} - 1) \text{ nA} \quad (129)$$

where $V_t = 25 \text{ mV}$, and the differential capacitance of the nonlinear capacitor was assumed to be of the form [32]

$$C_n(V_n) = \frac{5 \text{ pF}}{\sqrt{0.9 - V_n}} + e^{V_n/2V_t} \text{ pF} \quad (130)$$

where V_n is expressed in volts. Each nonlinear network is, essentially, a simplified model of a semiconductor diode. The line resistances are assumed to vary proportionally to the square root of frequency (the skin-effect variation), and their values at 1 MHz are assumed to be $R_{11} = R_{22} = 100 \Omega/\text{m}$ and $R_{12} = R_{21} = 10 \Omega/\text{m}$. The elements of the conductance matrix are assumed to be frequency-independent and equal to $G_{11} = G_{22} = 1 \text{ mS/m}$ and $G_{12} = G_{21} = -0.1 \text{ mS/m}$. The line response in this case is shown in Fig. 10, and it corresponds to taking a time step $\Delta t = 10 \text{ ps}$ in the convolution, and 1024 points in the frequency domain when computing Green's functions.

As the second example, we consider a transmission line having five signal conductors and a ground plane. The cross section of the line is sketched in Fig. 11. The line matrices $[L]$, $[B]$, $[R]$, and $[G]$ were computed using the techniques described in [33]–[37], yielding frequency-dependent values of these matrices. The line length was assumed to be 288 mm. The line was excited at the generator end of conductor number 1, by a $50-\Omega$ generator, the EMF of which is

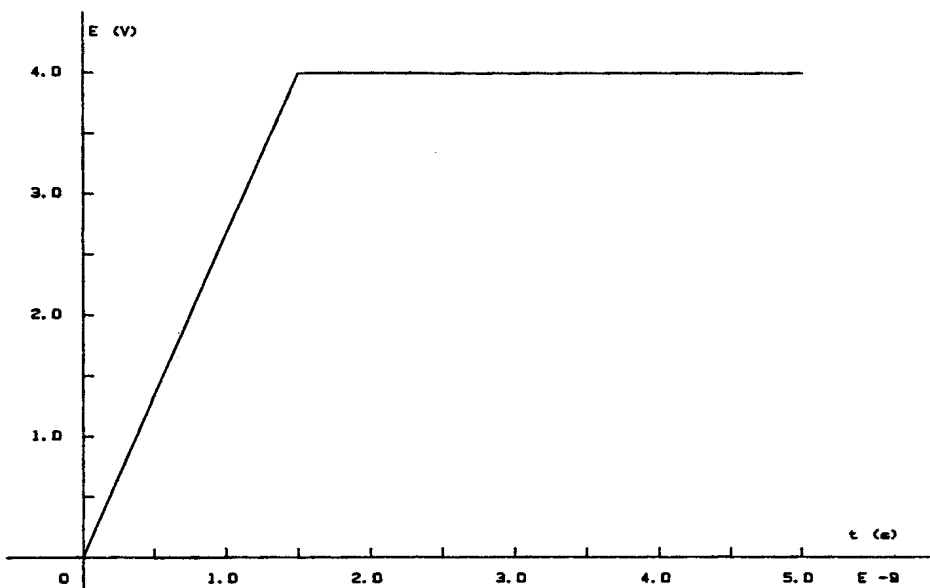


Fig. 6. Electromotive force of the voltage generator of Fig. 5.

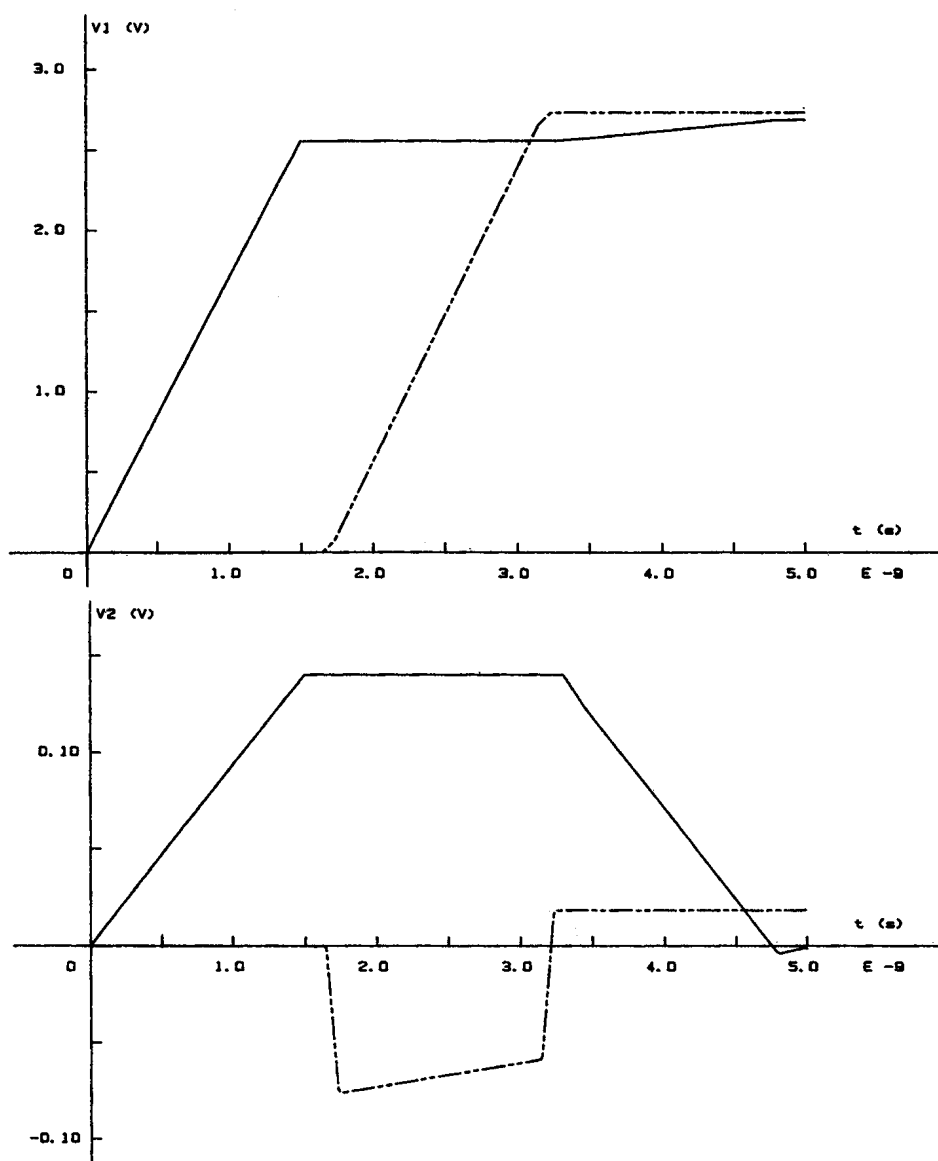


Fig. 7. Voltage waveforms at the terminals of the lossless transmission line of Fig. 5 obtained by modal analysis in time domain. — voltages at the generator end;
- - - voltages at the load end.

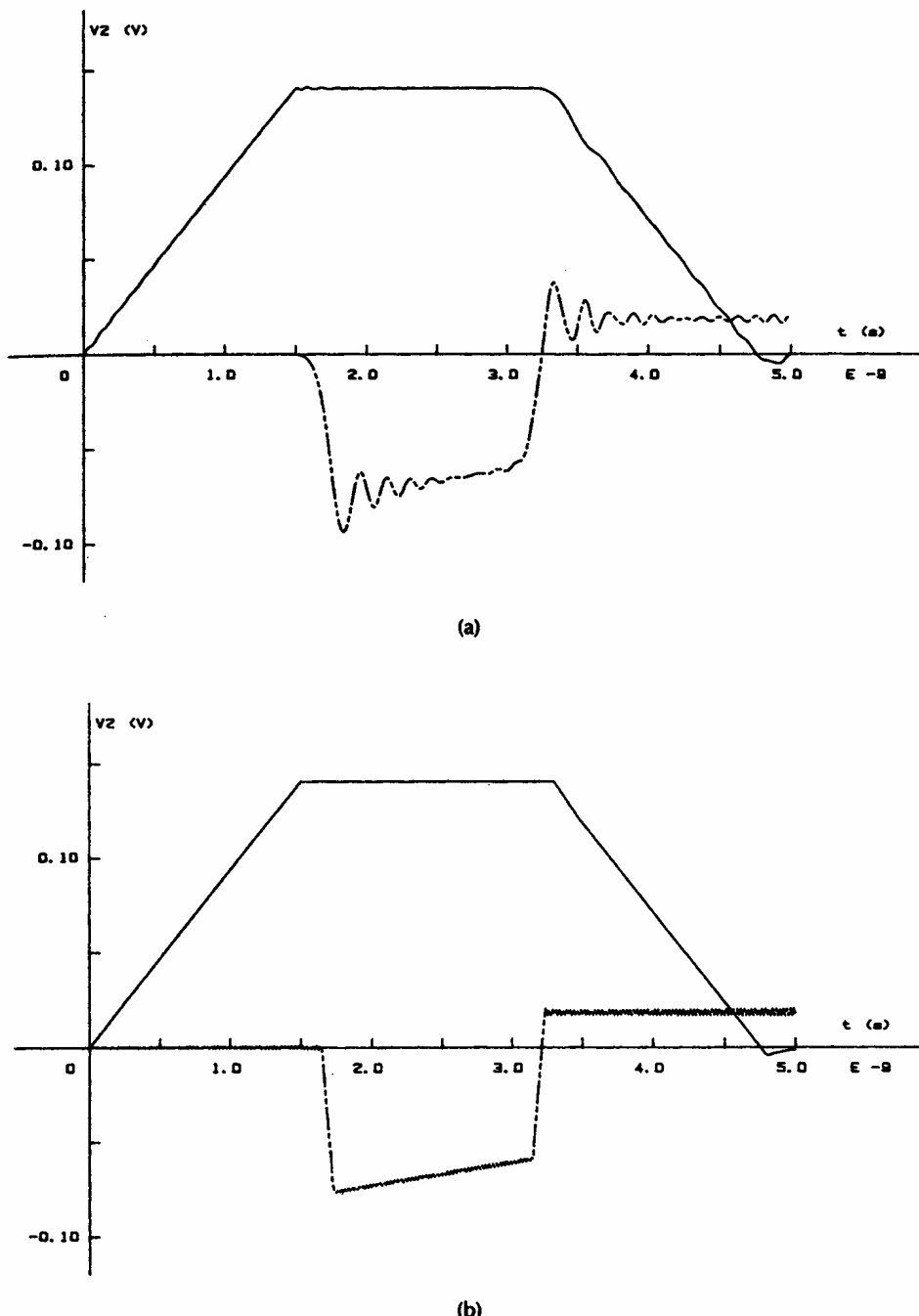


Fig. 8. Voltage waveforms at the terminals of the parasitic line of Fig. 5 obtained by (a) time-stepping solution, and (b) modal analysis in the frequency domain. — voltages at the generator end; - - - voltages at the load end.

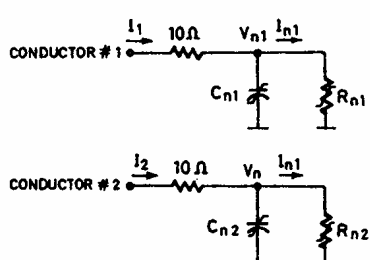


Fig. 9. Nonlinear RC load network for the transmission line of Fig. 5.

given by Fig. 12. All the other ports are connected to the ground through 50- Ω resistors. The response of the line was obtained by using modal analysis in the frequency domain, with 2048 time samples and a sampling frequency of 100 GHz. These results are presented in Fig. 13, together with experimental data for the same line. These results were obtained with a setup consisting of a Tektronix 7854 sampling oscilloscope, an S52 pulse generator, S4 and S6 sampling heads, and other auxiliary equipment, providing a bandwidth of 10 GHz. For a detailed description of the equipment refer to [38].

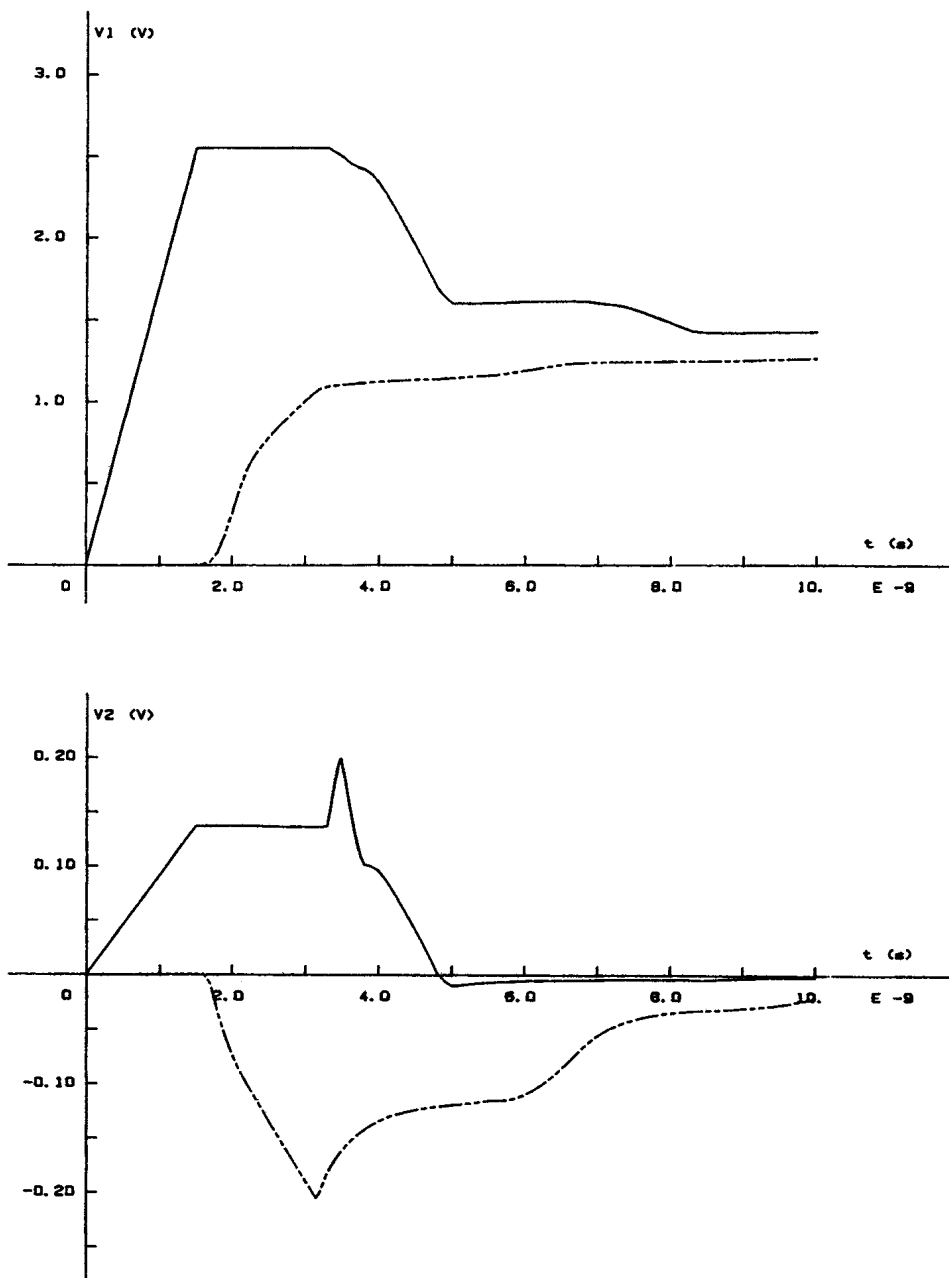


Fig. 10. Voltage waveforms at the terminals of the lossy transmission line of Fig. 5, terminated in the nonlinear RC load network of Fig. 9. — voltages at the generator end; - - - voltages at the load end.

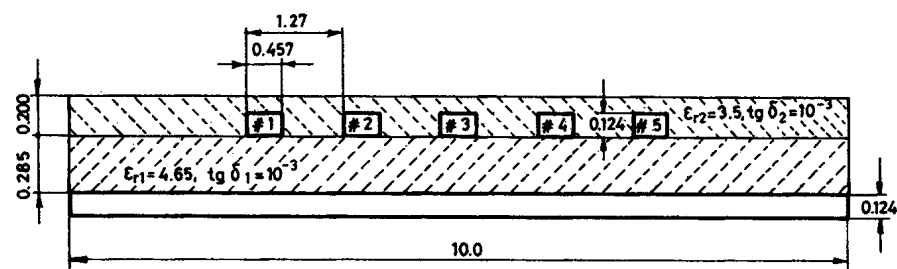


Fig. 11. Sketch of the cross section of a microstrip transmission line with five signal conductors. All dimensions are in millimeters.

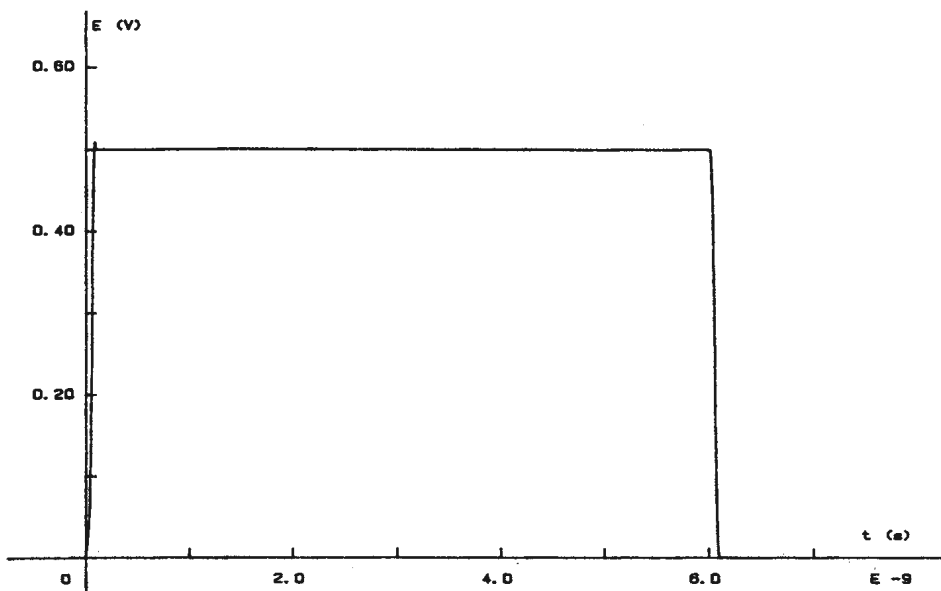
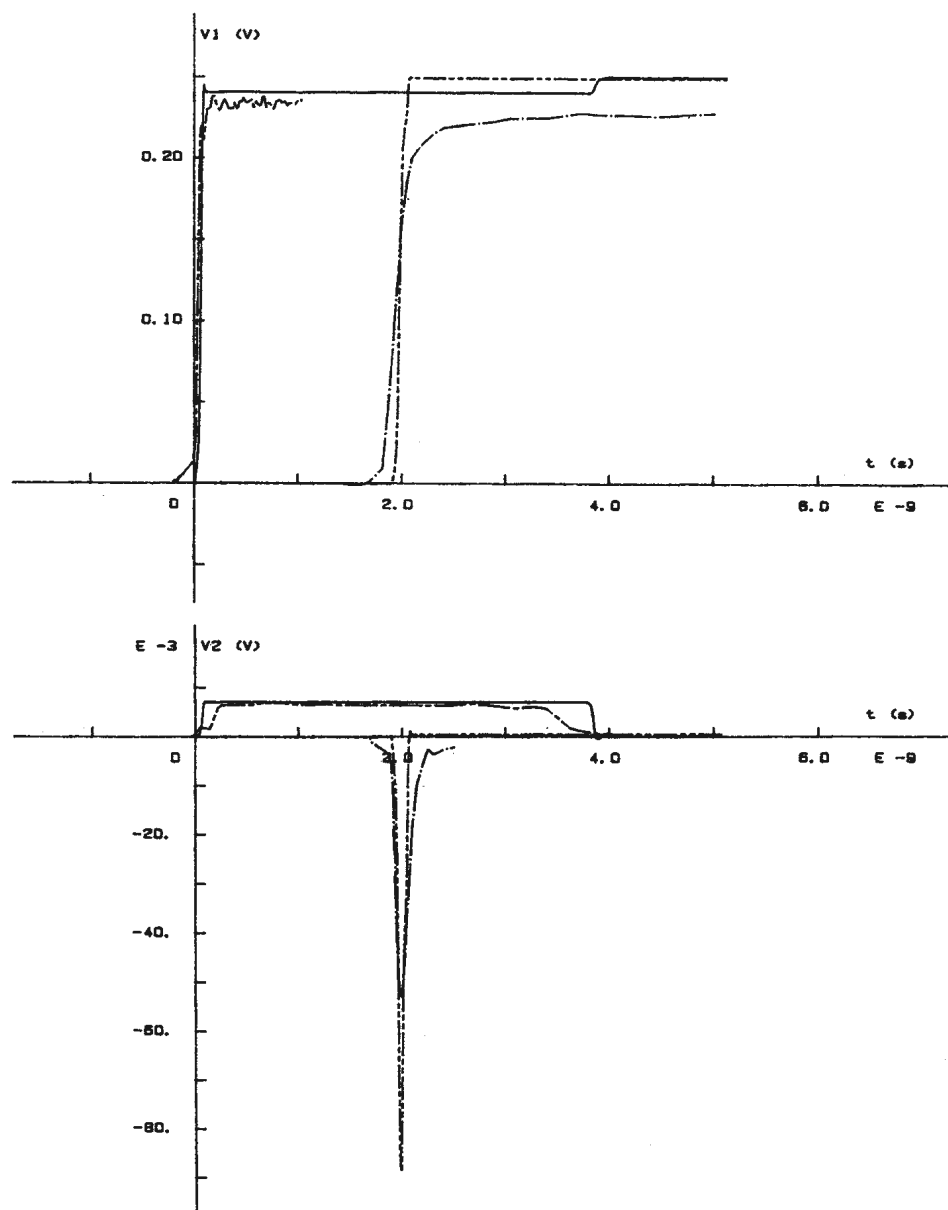


Fig. 12. Electromotive force of the voltage generator driving conductor #1 of the transmission line of Fig. 11.



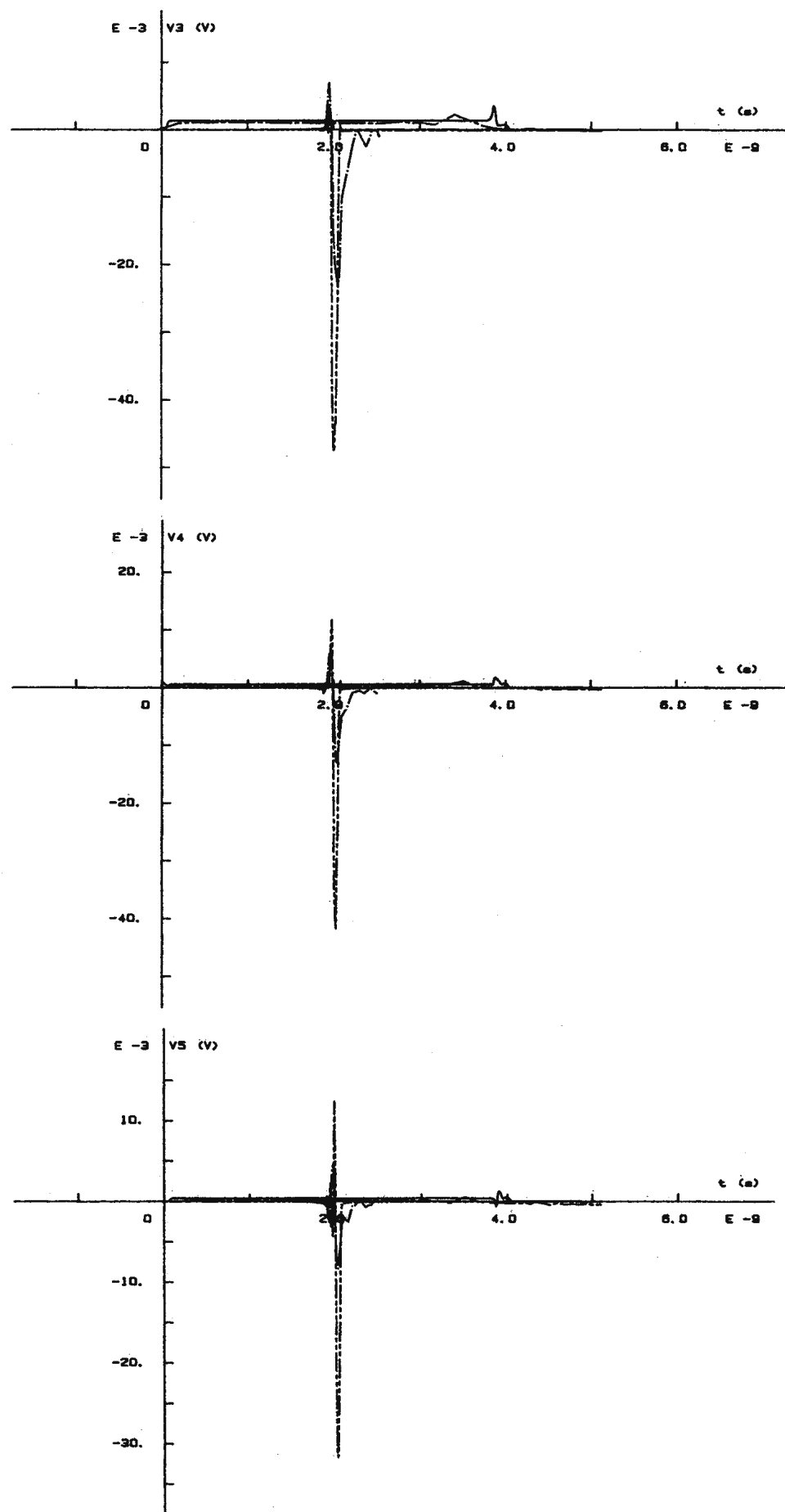


Fig. 13. Voltage waveforms at the terminals of the lossy transmission line of Fig. 11, terminated in 50Ω resistors at all ports. Voltages at the generator end: — theory; —— experiment. Voltages at the load end: - - - theory; - · - experiment.

Very good agreement between the theoretical and experimental results can be observed. The crosstalk between the conductors at the generator end is relatively small, because the coupling between the lines is loose. However, the crosstalk at the load end is significant, and results in sharp spikes. (Other spikes, of an opposite polarity, appear later, due to the trailing edge of the excitation waveform.) This crosstalk is due to the different velocities of propagation of the line eigenmodes. It is important to note that this crosstalk will increase if the line length is increased, or if the rise time of the pulse is decreased, up to a certain point, when the waveform of the crosstalk waveform becomes similar to that of Fig. 7 (at the load end of the parasitic line). After that, the crosstalk remains practically constant in amplitude.

In the design of certain computer buses, a number of conductors grounded at both line ends are introduced, with the intention to reduce crosstalk. In order to justify this practice, we have considered the same transmission line as above, but we have short-circuited the conductors number 2 and number 4 to the ground at the generator end and at the load end. The voltage waveforms at the driven port and at the other ports, terminated in 50Ω resistors, are given in Fig. 14. Comparing these diagrams to Fig. 13 we clearly see that the crosstalk at the load end has remained practically unchanged, while the crosstalk at the generator end has significantly increased! This has a very simple explanation. Namely, the presence of short-circuited conductors gives rise to a total of five eigenmodes (as opposed to three, as would be in the case if only conductors number 1, 3, and 5 were present). The dielectric of the line being inhomogeneous, these modes have different velocities of propagation. In the case where conductors number 2 and 4 are short-circuited to the ground, the line is poorly matched at both ends, and thus the waves are strongly reflected, which causes a crosstalk at the generator end after two line transit times. In contrast, if conductors number 2 and 4 are terminated in 50Ω resistors, the line is relatively well-matched, and the reflection is negligible. Note that the waveforms of Fig. 14 are polluted by the tails of the previous pulses introduced by the FFT.

Yet another interesting fact is that increasing the separation between the lines reduces only slightly the crosstalk for the structure shown in Fig. 11. Let us consider the line shown in Fig. 11, but with conductors number 2 and 4 "deleted," i.e., a line that consists of only three signal conductors and a ground plane. Assuming the line ports to be terminated in 50Ω loads, and keeping the same excitation as before, one obtains the line response shown in Fig. 15. Note that the crosstalk between adjacent lines (number 1 and 3 in the present case) at the generator end is smaller than for the previous case (for conductors number 1 and 2, as shown in Fig. 13). The reason is the smaller coupling between the adjacent lines, due to an increased distance between them. However, the crosstalk at the load end has remained practically unchanged. The explanation for this is simple—this crosstalk is due, in its major part, to the intra-modal dispersion (different modal propagation velocities), and this dispersion changes very slowly with increasing distance between the conductors. Only when the separation between the conductors becomes very large in terms of the conductor height above the ground plane will the intra-modal dispersion become small. However, such a case

seems to be impractical, and a much better remedy would be to provide a homogeneous dielectric for the bus.

VIII. CONCLUSIONS

Evaluation of the time-domain response of multiconductor transmission lines is of great importance in the analysis of crosstalk in fast digital circuit interconnections, as well as in the analysis of power lines.

In this paper, a few techniques were described which are useful for computation of the line response. We have assumed that the line circuit-theory parameters (i.e., the $[L]$, $[B]$, $[R]$, and $[G]$ matrices) are known, either from experimental data, or from an electromagnetic field analysis.

Starting from these quasi-TEM parameters, the telegrapher equations can be written for the multiconductor transmission line, and the wave equations can be derived. Together with any of these equations, a set of initial and boundary conditions must be defined to complete the set of equations for the line analysis.

The simplest method for evaluation of the time-domain response is a time-stepping solution of the telegrapher equations. This technique is based on discretizing the telegrapher equations in space and time, and it is equivalent to solving a lumped-circuit equivalent to the transmission line by the Euler method. The method is simple to implement on a computer. However, in order to obtain a good numerical solution, very fine subdivisions in both space and time are required, which make this procedure less efficient than the other methods presented in this paper. In addition, one has to carefully choose the time step, in order to provide a numerically stable solution. The advantage of the method is that it can easily be incorporated into the analysis of terminal networks, which can contain nonlinear elements, and it can treat lossy transmission lines, however only with frequency-independent parameters.

Modal analysis in the time domain is based on an eigenvalue equation which can be derived from the wave equation. This technique can only be applied to lossless lines (with frequency-independent parameters), but it is the fastest technique, and being performed in the time domain, it can easily be interfaced to the analysis of terminal networks (which can contain nonlinear elements). The line eigenmodes propagate along the (lossless) line without dispersion (assuming the quasi-TEM mode of propagation only), and for the tracking of these modes one has to store only samples of the line voltages at the two terminals, over a time interval equal to the line transit time.

Modal analysis in the frequency domain is similar to the previous technique, except that it is performed in the frequency domain. This technique can treat lossy lines (i.e., it can include skin-effect and dielectric losses), which, generally, have frequency-dependent parameters. However, the terminal networks must contain only linear elements, because nonlinear networks cannot, in general, be analyzed in the frequency domain. The Fourier transform (more precisely, the fast Fourier transform) is used to change between the time domain and the frequency domain. This technique is less efficient with regard to the CPU time than the modal analysis in time domain, but, usually, it is more efficient than the time-stepping solution.

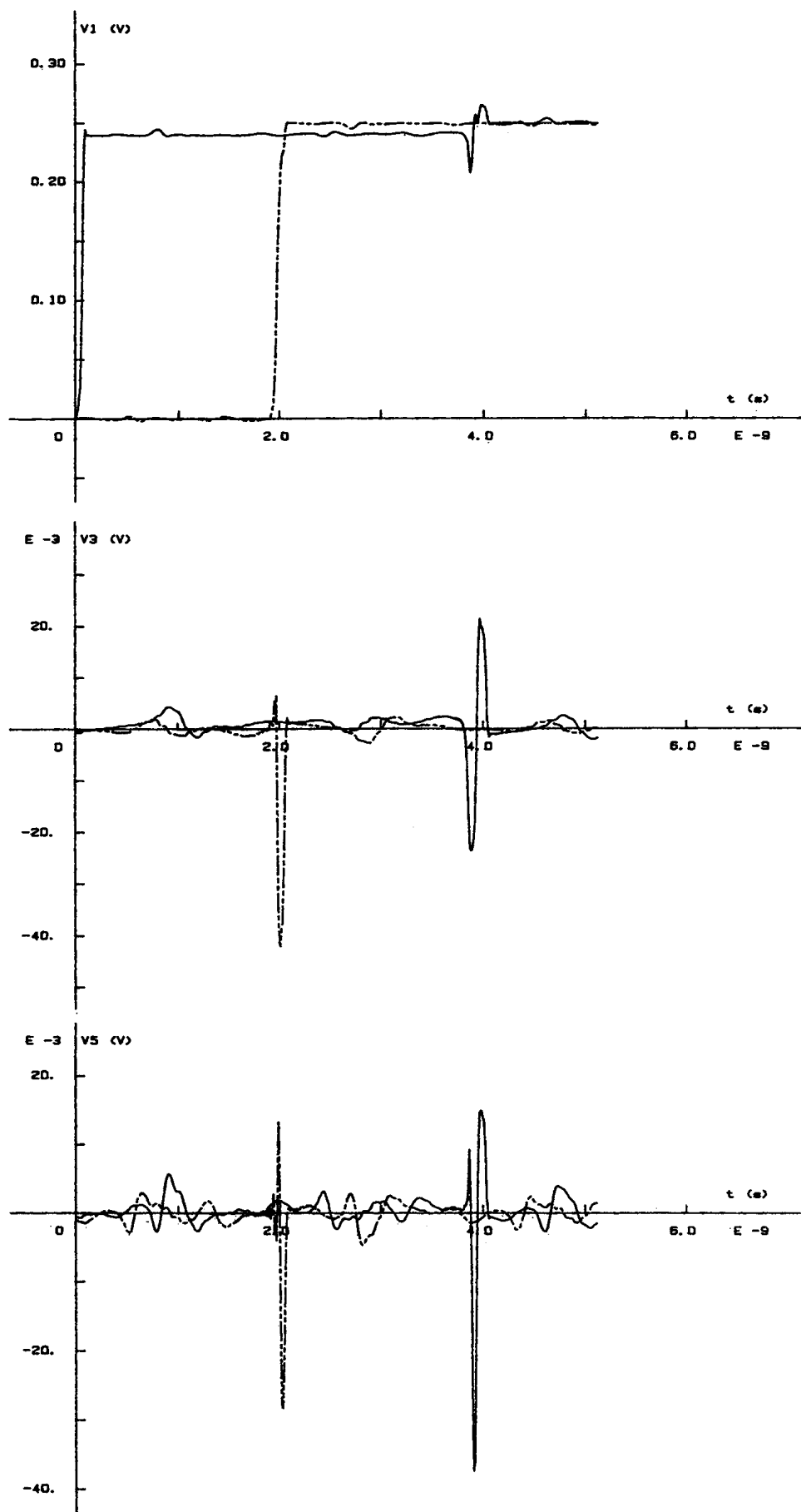


Fig. 14. Voltage waveforms at the terminals of the lossy transmission line of Fig. 11, with conductors #2 and #4 short-circuited at both ends. — voltages at the generator end; - - - voltages at the load end.

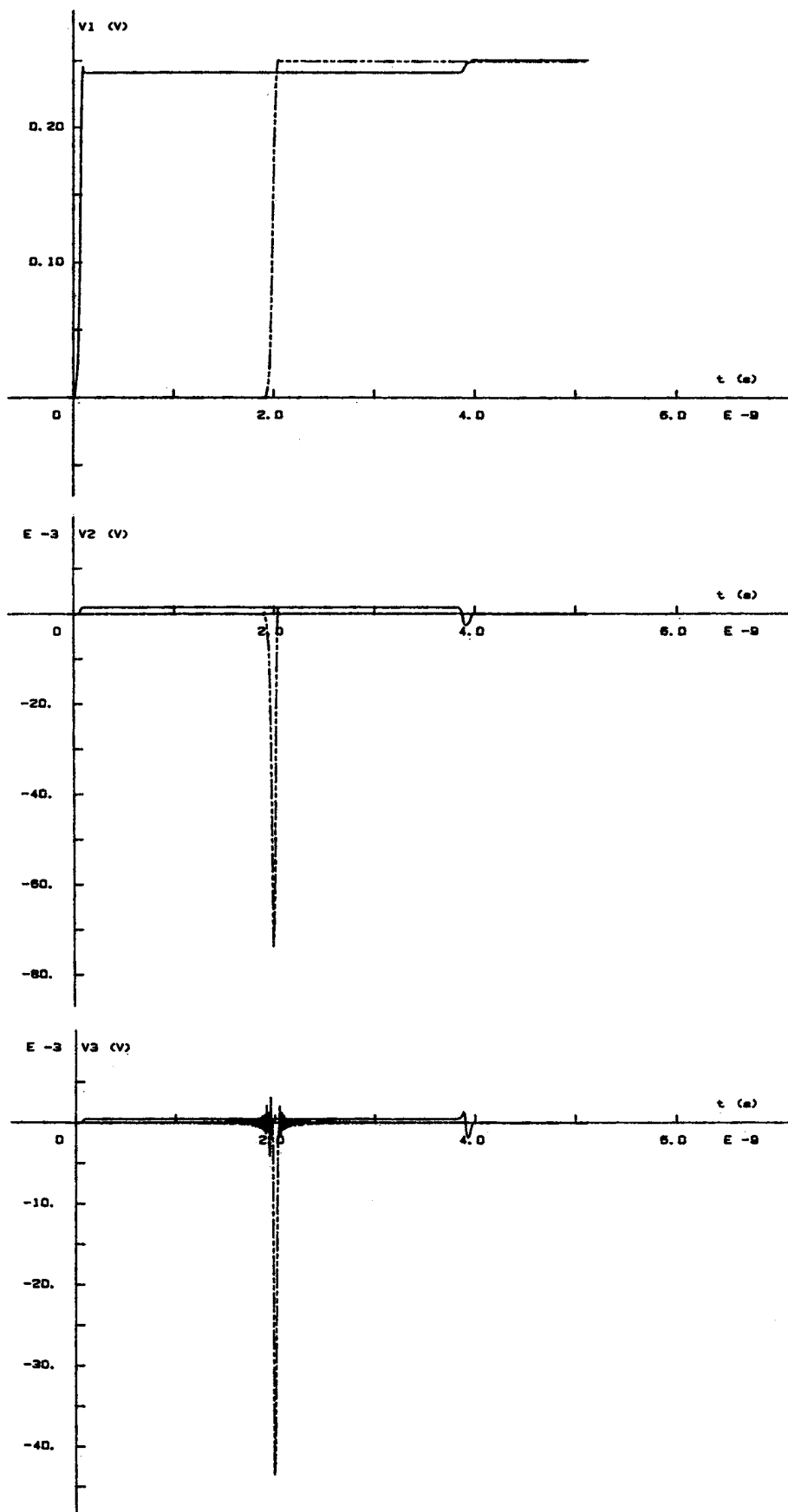


Fig. 15. Voltage waveforms at the terminals of a lossy transmission line with three signal conductors, coinciding with conductors #1, #3, and #5 of the transmission line of Fig. 11, terminated in 50Ω resistors at all ports. — voltages at the generator end; - - - voltages at the load end.

In the analysis of digital circuits, the terminal networks are often nonlinear, and line losses cannot be neglected if the line length is relatively large. The last technique presented in this paper is capable of treating such general cases. It is based on an evaluation of line Green's functions (i.e., line responses to delta-function excitations). In order to make the computation of these functions efficient, the line should be terminated in suitable resistances, which make the line impulse response settle down fast, thus requiring a relatively short storage for Green's functions to expedite the computations. Green's functions are evaluated by using the modal analysis in the frequency domain, and the fast Fourier transform. Green's functions are then convolved with the line port voltages under the assumption that real terminal networks are connected to the line. This method can treat the most general case of quasi-TEM multiconductor transmission lines with arbitrary terminations, but it is substantially slower than the modal analyses, and slightly superior to the time-stepping solution.

Finally, examples are given to illustrate the various techniques for the multiconductor transmission line analysis. For a given lossless transmission line with two signal conductors, the response is evaluated by using all the present techniques. The results compare very well with each other. Modal analysis in the time domain gives the sharpest waveforms, the convolution technique is next, modal analysis in the frequency domain yields small oscillations in the response (due to aliasing which is inherent to the fast Fourier transform), and waveforms obtained by the time-stepping solution have the largest spurious oscillations. The second example is a transmission line with five signal conductors made by a printed-circuit technique. The response of this line was both computed and measured, and the two sets of results agree very well. Crosstalk between the conductors was considered. It was shown that the crosstalk at the near (generator) end is due to the coupling between the lines, and it decreases when the line separation is increased. Crosstalk at the far (load) end is primarily due to the intra-modal dispersion (i.e., different group velocities of the line eigenmodes), and it can most efficiently be reduced by making the line dielectric homogeneous. Of course, crosstalk also depends strongly on the terminations at both line ends. It was also demonstrated that insertion of end-grounded conductors between the signal conductors does not reduce the crosstalk at the far end at all, and may significantly increase the crosstalk at the near end.

ACKNOWLEDGMENT

The authors would like to thank Dr. R. Heinz, who skillfully performed the measurements, part of which were presented in this paper, and to Dr. J. Venkataraman, who performed the computation of the multiconductor transmission line circuit parameters for the line used in the measurements.

REFERENCES

- [1] A. J. Poggio and E. K. Miller, "Integral equation solution of three-dimensional scattering problems," in R. Mittra, Ed., *Computer Techniques for Electromagnetics*. Oxford, England: Pergamon, 1973.
- [2] T. C. Edwards, *Foundations for Microstrip Circuit Design*. Chichester, England: Wiley, 1981, ch. 5.
- [3] S. Frankel, *Multiconductor Transmission Line Analysis*. Dedham, MA: Artech House, 1977.
- [4] O. Heaviside, *Electromagnetic Theory, Vol. 1 (reprint)*. New York, NY: Dover, 1950.
- [5] G. A. Campbell, "Dr. Campbell's memoranda of 1907 and 1912," *Bell Syst. Tech. J.*, vol. 14, pp. 558-572, Oct. 1935.
- [6] L. A. Pipes, "Matrix theory of multiconductor transmission lines," *Phil. Mag.*, vol. 24, pp. 97-113, July 1937.
- [7] S. O. Rice, "Steady state solutions of transmission line equations," *Bell Syst. Tech. J.*, vol. 24, pp. 131-178, Apr. 1941.
- [8] M. Cotte, "Theorie de la Propagation d'ondes de choc sur deux lignes parallèles," *Rev. Gen. Elec.*, vol. 56, pp. 343-350, 1947.
- [9] S. A. Schelkunoff, "Conversion of Maxwell's equations into generalized telegrapher's equations," *Bell Syst. Tech. J.*, vol. 34, pp. 995-1043, Sept. 1955.
- [10] D. B. Jarvis, "The effects of interconnections on high-speed logic circuits," *IEEE Trans. Electromag. Compat.*, vol. EC-12, pp. 476-487, Oct. 1963.
- [11] L. M. Wedepohl, "Application of matrix methods to the solution of travelling wave phenomena in polyphase systems," *Proc. Inst. Elec. Eng.*, vol. 110, pp. 2200-2212, Dec. 1963.
- [12] —, "Electrical characteristics of polyphase transmission systems with special reference to boundary-value calculations at power-line carrier frequencies," *Proc. Inst. Elec. Eng.*, vol. 112, pp. 2103-2212, Nov. 1965.
- [13] H. Amemiya, "Time domain analysis of multiple parallel transmission lines," *RCA Rev.*, pp. 241-276, June 1967.
- [14] H. Uchida, *Fundamentals of Coupled Lines and Multiwire Antennas*. Sendai, Japan: Sasaki Publ., 1967.
- [15] L. M. Wedepohl and S. E. T. Mohamed, "Multiconductor transmission lines—Theory of natural modes and Fourier integral applied to transient analysis," *Proc. Inst. Elec. Eng.*, vol. 116, pp. 1553-1563, Sept. 1969.
- [16] A. Budner, "Introduction of frequency dependent line parameters into an electromagnetic transients program," *IEEE Trans. Power App. Syst.*, vol. PAS-89, pp. 88-97, Jan. 1970.
- [17] L. M. Wedepohl and S. E. T. Mohamed, "Transient analysis of multiconductor transmission lines with special reference to nonlinear problems," *Proc. Inst. Elec. Eng.*, vol. 17, pp. 979-988, May 1970.
- [18] F. Y. Chang, "Transient analysis of lossless coupled transmission lines in a non-homogeneous dielectric medium," *IEEE Trans. Microwave Theory Tech.*, vol. MTT-18, pp. 616-626, Sept. 1970.
- [19] M. K. Krage and G. I. Haddad, "Characteristics of coupled microstrip transmission lines with inhomogeneous dielectrics," *IEEE Trans. Microwave Theory Tech.*, vol. MTT-20, pp. 678-688, Oct. 1972.
- [20] K. D. Marx, "Propagation modes, equivalent circuits, and characteristic terminations for multiconductor transmission lines with inhomogeneous dielectrics," *IEEE Trans. Microwave Theory Tech.*, vol. MTT-21, pp. 450-457, July 1973.
- [21] C. R. Paul, "On uniform multimode transmission lines," *IEEE Trans. Microwave Theory Tech.*, vol. MTT-21, pp. 556-558, Aug. 1973.
- [22] G. L. Wilson and K. A. Schmidt, "Transmission line models for switching studies: design criteria, part II. Selection of section length, model design and tests," *IEEE Trans. Power App. Syst.*, vol. PAS-93, pp. 389-395, Jan. 1974.
- [23] W. S. Meyer and H. W. Domme, "Numerical modelling of frequency-dependent transmission parameters in an electromagnetic transient program," *IEEE Trans. Power App. Syst.*, vol. PAS-93, pp. 1401-1409, Sept. 1974.
- [24] R. Brieche, "Analyse von Kammleitungsfiltern un ähnlichen Baugruppen aus gekoppelten Mehrlietersystemen," *Frequenz*, vol. 29, pp. 94-99, Apr. 1975.
- [25] C. R. Paul, "Useful matrix chain parameter identities for the analysis of multiconductor transmission lines," *IEEE Trans. Microwave Theory Tech.*, vol. MTT-23, pp. 756-760, Sept. 1975.
- [26] A. Anetani, "A highly efficient method for calculating transmission line transients," *IEEE Trans. Power App. Syst.*, vol. PAS-95, pp. 1545-1551, Sept. 1976.
- [27] D. M. Triezenberg, "An efficient state variable transmission line model," *IEEE Trans. Power App. Syst.*, vol. PAS-98, pp. 484-492, Mar. 1979.
- [28] A. J. Groudis and C. S. Chang, "Coupled lossy transmission line characterization and simulation," *IBM J. Res. Develop.*, vol. 25, pp. 25-41, Jan. 1981.
- [29] R. W. Lorenz, "Über Lecher-Wellen, Leitungs-Wellen und

- TEM-Wellen auf verlustbehafteten Mehrleitersystemen und die Bedeutung der Diffusionsgleichung zur Ermittlung der Leitungsbeläge," *Frequenz*, vol. 25, pp. 208-214, July 1971.
- [30] IMSL Library, Houston, TX: IMSL.
- [31] A. R. Djordjević, T. K. Sarkar, and R. F. Harrington, "Analysis of lossy transmission lines with arbitrary nonlinear terminal networks," *IEEE Trans. Microwave Theory Tech.*, vol. MTT-34, pp. 660-666, June 1986.
- [32] J. Millman and Ch.C. Halkias, *Integrated Electronics*. Tokyo, Japan: McGraw-Hill, 1972, chs. 3 and 19.
- [33] C. Wei, R. F. Harrington, J. R. Mautz, and T. K. Sarkar, "Multiconductor transmission lines in multilayered dielectric media," *IEEE Trans. Microwave Theory Tech.*, vol. MTT-32, pp. 439-450, Apr. 1984.
- [34] R. F. Harrington and C. Wei, "Losses on multiconductor transmission lines in multilayered dielectric media," *IEEE Trans. Microwave Theory Tech.*, vol. MTT-32, pp. 705-710, July 1984.
- [35] S. M. Rao, T. K. Sarkar, and R. F. Harrington, "The electrostatic field of conducting bodies in multiple dielectric media," *IEEE Trans. Microwave Theory Tech.*, vol. MTT-32, pp. 1441-1448, Nov. 1984.
- [36] J. N. Venkataraman, S. M. Rao, A. R. Djordjević, T. K. Sarkar, and Y. Naiheng, "Analysis of arbitrarily oriented microstrip transmission lines in arbitrarily shaped dielectric media over a finite ground plane," *IEEE Trans. Microwave Theory Tech.*, vol. MTT-33, pp. 952-959, Oct. 1985.
- [37] A. R. Djordjević, T. K. Sarkar, and S. M. Rao, "Analysis of finite-conductivity cylindrical conductors excited by axially-independent TM electromagnetic field," *IEEE Trans. Microwave Theory Tech.*, vol. MTT-33, pp. 960-966, Oct. 1985.
- [38] F. I. Tseng and T. K. Sarkar, "Experimental determination of resonant frequencies by transient scattering from conducting cylinders," *IEEE Trans. Antennas Propagat.*, vol. AP-32, pp. 914-918, Sept. 1984.



Antonije R. Djordjević was born in Belgrade, Yugoslavia, in 1952. He received the B.Sc., M.Sc., and D.Sc. degrees from the University of Belgrade in 1975, 1977, and 1979, respectively. In 1975 he joined the Department of Electrical Engineering, University of Belgrade, as a Teaching Assistant in Electromagnetics. In 1982 he was appointed as Assistant Professor in Microwaves at the same department. From February 1983 until February 1984 he was with the Department of Electrical Engineering, Rochester Institute of Technology, Rochester, NY, as a Visiting Associate Professor. His research interests are numerical problems in electromagnetics, especially those applied to antennas and microwave passive components.



Tapan K. Sarkar (Senior Member, IEEE) was born in Calcutta, India, on August 2, 1948. He received the B. Tech. degree from the Indian Institute of Technology, Kharagpur India, in 1969, the M.Sc.E. degree from the University of New Brunswick, Frederickton, NB, Canada, in 1971, and the M.S. and Ph.D. degrees from Syracuse University Syracuse, NY, in 1975.

From 1969 to 1971, he served as an Instructor at the University of New Brunswick. While studying at the Syracuse University, he served as an Instructor and Research Assistant in the Department of Electrical and Computer Engineering. From 1976 to 1985, he was with Rochester Institute of Technology, Rochester, NY. From 1977 to 1978 he was a Research Fellow at the Gordon McKay Laboratory at Harvard University, Cambridge, MA. Currently, he is associated with Syracuse University. His research interests deal with numerical solution of operator equations arising in electromagnetics and signal processing.

Dr. Sarkar is an associate editor of *IEEE TRANSACTIONS ON ELECTROMAGNETIC COMPATIBILITY*, associate editor for feature articles for *IEEE ANTENNAS AND PROPAGATION NEWSLETTER*, and on the editorial board of *Journal of Electromagnetic Waves and Applications*. He is also Vice Chairman of the URSI international commission on Time Domain Metrology. He is a member of Sigma Xi, URSI Commissions A and B, and a Registered Professional Engineer in the State of New York.



Roger F. Harrington (Fellow, IEEE) was born in Buffalo, NY, on December 24, 1925. He received the B.E.E. and M.E.E. degrees from Syracuse University, Syracuse, NY, in 1948 and 1950, respectively, and the Ph.D. degree from Ohio State University, Columbus, OH, in 1952.

From 1945 to 1946, he served as an Instructor at the U.S. Naval Radio Material School, Dearborn, MI, and from 1948 to 1950, he was employed as an Instructor and Research Assistant at Syracuse University. While studying at Ohio State University, he served as a Research Fellow in the Antenna Laboratory. Since 1952, he has been on the faculty of Syracuse University, where he is presently Professor of Electrical Engineering. During 1959-1960 he was Visiting Associate Professor at the University of Illinois, Urbana, in 1964 he was Visiting at the University of California, Berkeley, in 1969 he was Guest Professor at the Technical University of Denmark, Lyngby, and in 1983 he was Visiting Professor at the East China Normal University.

Dr. Harrington is a member of Tau Beta Pi, Sigma Xi, the American Association of University Professors, and the International Union of Radio Science.